Distribution Agreement

In presenting this thesis as a partial fulfillment of the requirements for a degree from Emory University, I hereby grant to Emory University and its agents the non-exclusive license to archive, make accessible, and display my thesis in whole or in part in all forms of media, now or hereafter now, including display on the World Wide Web. I understand that I may select some access restrictions as part of the online submission of this thesis. I retain all ownership rights to the copyright of the thesis. I also retain the right to use in future works (such as articles or books) all or part of this thesis.

Drason Zhang April 7, 2023

Carboxylation of C(sp^2) Bromides Enabled by Metallophotoredox Dual Catalysis and Sodium Formate

By

Drason Zhang

Dr. William Wuest
Adviser

Chemistry

Dr. William Wuest

Adviser

Dr. Matthew Weinschenk

Committee Member

Dr. Richard Himes

Committee Member

2023

Carboxylation of C(sp^2) Bromides Enabled by Metallophotoredox Dual Catalysis and Sodium Formate

By

Drason Zhang

Dr. William Wuest

Adviser

An abstract of
a thesis submitted to the Faculty of Emory College of Arts and Sciences
of Emory University in partial fulfillment
of the requirements of the degree of
Bachelor of Science with Honors

Chemistry

2023

Abstract

Carboxylation of C(sp^2) Bromides Enabled by Metallophotoredox Dual Catalysis and Sodium Formate

By Drason Zhang

In recent years, photoredox-mediated processes have seen a resurgence in popularity due to their ability to enable novel reactivity via pathways involving thermally inaccessible intermediates. These photoredox processes include single-electron transfer and energy transfer processes, which are attractive due to their ability to occur under mild conditions that enable high functional group tolerance. Previous work has developed formate salts as precursors to the carbon dioxide radical anion ($CO_2^{\bullet-}$) via hydrogen-atom transfer (HAT) under photochemical conditions; this radical anion was shown to undergo a variety of processes, including Giese-type addition to electron-deficient olefins. Given this, our group wondered if $CO_2^{\bullet-}$ could instead be leveraged as a partner in C-C bond formation cross-coupling, which would enable facile access to carboxylic acids: a common organic functional group in natural products, pharmaceutical agents, and more. This report focuses on the successful development of such a method that leverages a metallophotoredox/HAT triple catalysis reaction manifold: utilizing visible light, 4CzIPN, nickel, and formate salts as a source of $CO_2^{\bullet-}$, we are able to construct a wide variety of carboxylic acids bearing diverse functional groups from simple (hetero)aryl or vinyl C(sp^2)-bromide starting materials. Of note, we report that catalytic amounts of *N*-phenyl-bis(trifluoromethanesulfonamide) play an essential role in carboxylation. Overall, we have developed a mild method enabling facile access to carboxylic acids from readily available starting materials.

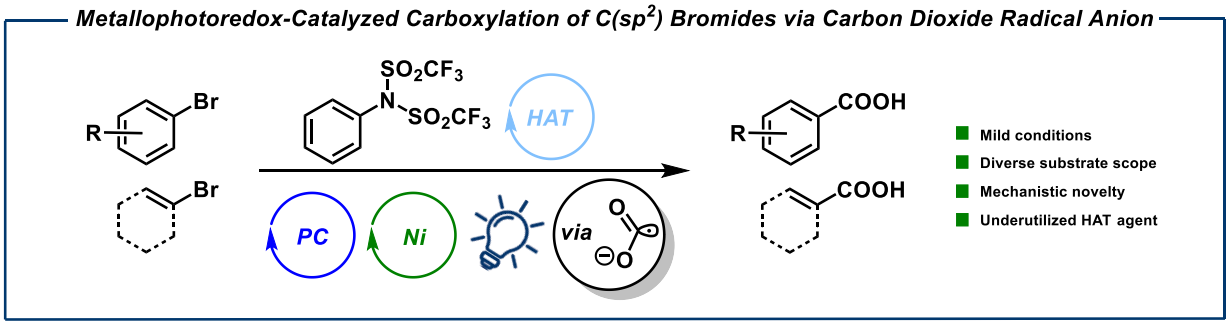

Carboxylation of C(sp^2) Bromides Enabled by Metallophotoredox Dual Catalysis and Sodium Formate

By

Drason Zhang

Dr. William Wuest
Adviser

A thesis submitted to the Faculty of Emory College of Arts and Sciences
of Emory University in partial fulfillment
of the requirements of the degree of
Bachelor of Science with Honors

Chemistry

2023

ACKNOWLEDGEMENTS

Bill: thank you for taking a chance on me and allowing me to pursue organic chemistry in your lab. It means so much to me that you have always been encouraging and supportive of my endeavors, be it fluctuating career goals or research interests or the various awards, scholarships, and fellowships that I have applied to. Thank you also for your guidance throughout my undergraduate career as I stumbled through course selection and graduate school applications. Without the chance you have given me I may never have realized my passion for synthetic chemistry and followed my original plans to become a biochemist! I look forward to continuing my earnest pursuit of organic chemistry and its widespread application; I hope you can look forward to my future independent career.

Dr. Weinschenk: thank you for always being willing to answer questions about chemistry and for allowing me to be your LA for 203 and 322. It is always a pleasure to listen to your lectures, and I always feel that I learn something new.

Dr. Himes: I always love seeing you walk through Atwood and am endlessly appreciative of our brief conversations about life when we meet; thank you for teaching me about analytical chemistry and for being such a fun person to talk to.

To the Wuest lab: Thank you so much for your friendship and mentorship in these past couple of years. I have learned so much from all of you; but perhaps more importantly, throughout the pandemic, when I was unable to return to China to visit my parents, you all helped make the lab feel like a home I could always be comfortable in. For that, I am eternally grateful; I think my sanity may have slipped a bit if not for you all. I will also formally apologize to Andrew, Christian, Elise, and Germán for constantly bothering you guys in your office…

Gavin, thank you for guiding my first steps as a methods chemist. You have taught me so much about how to think about reactivity and the different factors one might consider in the process of optimizing a reaction. Thank you for your friendship and for the endless banter; you have helped make my last year at Emory so special.

Christian and Andrew, thank you for first teaching me how to set up and run reactions. Thanks for being my first friends in the lab and for all the philosophical, nonsensical, and at times educational conversations; you were instrumental in developing my interest in organic synthesis.

Of course, I have to thank the other Wuest Lab Wondergrads for their support, friendship, and kindness as well. Sorry for unofficially claiming one of the desks in the office… I promise I'll move all my papers and books.

And without the support of my family, I would never have had the opportunity to come to Emory and come as far as I have. Thank you to my parents, Haizhen and Paul, and my sister, Connie. Thank you also to my 奶奶; I know you worried about my lack of motivation often in high school. I've turned that around and I hope that I've been able to make you proud. Keep watching over me; I will strive to continue making you proud.

Table of Contents

Figures

Chapter 1: Shining Light on Photoredox Methods

1.1 A Brief Discussion on the Development of Synthetic Methods

"The desire to translate a strategy to a reality can serve as a powerful impulse to explore new chemistry to close the gaps identified by the analysis."

—S. J. Danishefsky[1]

At the inception of chemical synthesis as a field, the methods available to chemists were limited to simple nucleophile-electrophile transformations (**Fig. 1A**).[2] Though simple by today's standards, this kind of reactivity enabled a number of impressive total syntheses, including R. B. Woodward's seminal synthesis of strychnine in 1954.[3] This achievement must not be understated; Sir Robert Robinson remarked that "for its molecular size it is the most complex substance known," emphasizing the challenge surmounted through the efforts of Woodward's group.[4] Note, however, that often early syntheses were undertaken to confirm the structure of a complex natural product, explaining why only simple and well-understood reactions were used.[2]

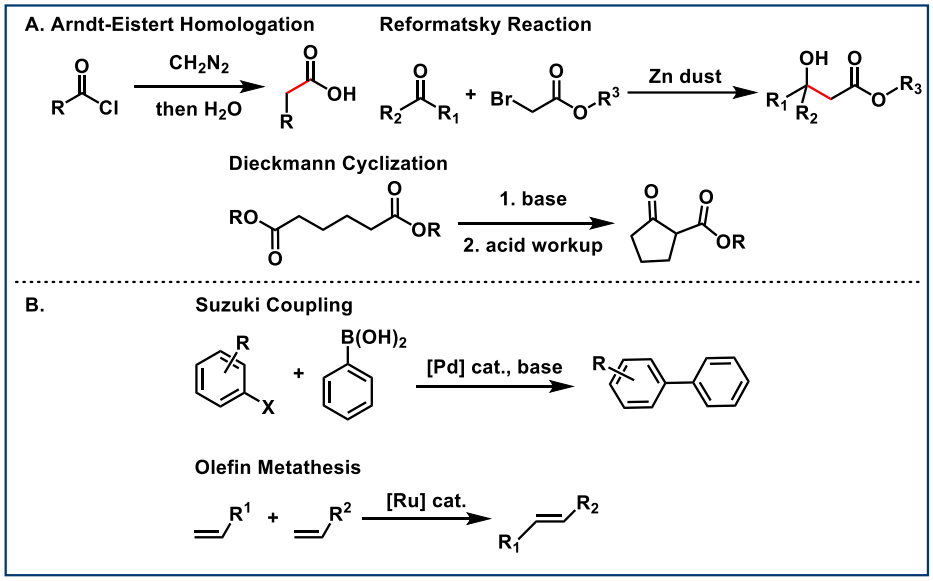

Figure 1. (a) Selected examples of early synthetic methods. (b) Selected examples of transition metal catalysis.

The advent of modern spectroscopic techniques in the early-mid 1900s enabled a departure from this paradigm; a combination of UV/vis, infrared, and mass spectroscopy provided key information about the structure of isolated natural products. The development of NMR spectroscopy in the 1960s in combination with crystallographic techniques completed the

modern panacea for structural elucidation, opening up the field of synthetic chemistry towards the challenge of developing new methods, identifying unique reactivity patterns, and applying one's creativity to the synthesis of a target. In the words of Reinhard Hoffman: "Synthesis itself became an object of research: the way is the goal."[2]

In such a setting, many powerful methods have been developed, enabling a variety of bond disconnections useful in synthesis; one shining example is transition metal catalysis, enabling powerful carbon-carbon bond formations through methods like olefin metathesis or Suzuki coupling (**Fig. 1B**).[2] Many other examples can be found in the myriad fields ranging from electrochemistry to organocatalysis to photoredox catalysis. Of particular relevance to this work is the latter, which has proven itself to be an incredibly powerful tool for accessing small molecule activation.[5–12]

1.2 An Introduction to Visible Light Photoredox Catalysis

"The goal is always finding something new, hopefully unimagined, and better still, hitherto unimaginable."

—K. B. Sharpless[13]

Though the field of catalysis is broad, encompassing numerous subfields, one uniting feature is the overarching goal of enabling novel pathways of reactivity. One subfield that meets this goal extremely well is that of photoredox catalysis, wherein visible light excitation enables generation of reactive intermediates that are thermally inaccessible.[5,6] Such reactivity stems from the ability of polypyridyl ruthenium or iridium complexes and organic dyes (known collectively as photocatalysts) to "exchange" visible light energy for chemical energy via electronic excitation, resulting in an excited state that can undergo single-electron transfer (SET) processes with other organic molecules or organometallic complexes. [5–12]

Consider the characteristics of $Ru(bpy)_3^{2+}$ as a model for other transition metal photocatalysts: under visible light, the species absorbs a photon, causing the excitation of a metal-centered *d*-orbital electron to an empty bipyridyl ligand π^* orbital (a process termed metal-to-ligand charge transfer, MLCT).[14,15] This occurs rather than excitation from a t_{2g} orbital to an e_g orbital, due to the Laporte orbital selection rule which forbids $d \rightarrow d$ transitions. Similarly, electronic selection rules dictate that the excited state must be in the singlet spin state; rapid intersystem crossing causes the formation of a lower energy triplet spin excited state, which is sufficiently long-lived to engage in single-electron transfer processes.[5,6,15,16] As a unique feature of the excited state, $*Ru(bpy)_3^{2+}$ is both more oxidizing and more reducing than the ground state: a low-energy hole in the t_{2g} orbital allows the excited state to accept an electron, while the occupied high energy π^* easily donates an electron. Such characteristics enable pathways that proceed through oxidative and reductive quenching of the excited state (**Scheme 1**).[5,6,17]

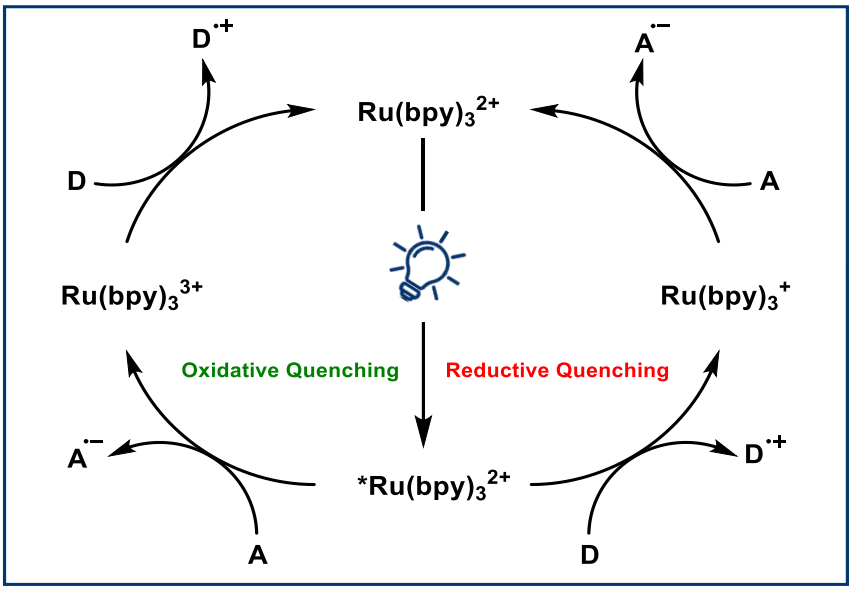

Scheme 1. Oxidative and reductive quenching pathways of $*Ru(bpy)_3^{2+}$. Scheme adapted from Prier et al. (2013).[6]

Notably, it has been demonstrated that many organic compounds are also capable photocatalysts, providing easily accessible, inexpensive, and ultimately more sustainable

alternatives to the prototypical ruthenium and iridium photocatalysts.[9,18–21] Similarly to transition metal photocatalysts, these organic photocatalysts rely on an appropriately long-lived triplet excited state that allows for non-radiative photoinduced electron transfer pathways, undergoing similar reductive or oxidative quenching cycles to that of $Ru(bpy)_3^{2+}$ (*vide supra*).[9,22]

The uniquely powerful chemistry of these photocatalysts has been leveraged for a diverse array of transformations. This stunning level of variety can be illustrated by the seminal reports of photoredox catalysis from the groups of Yoon, MacMillan, and Stephenson, demonstrating the application of photoredox to different reaction types (**Figure 2**).[23–25]

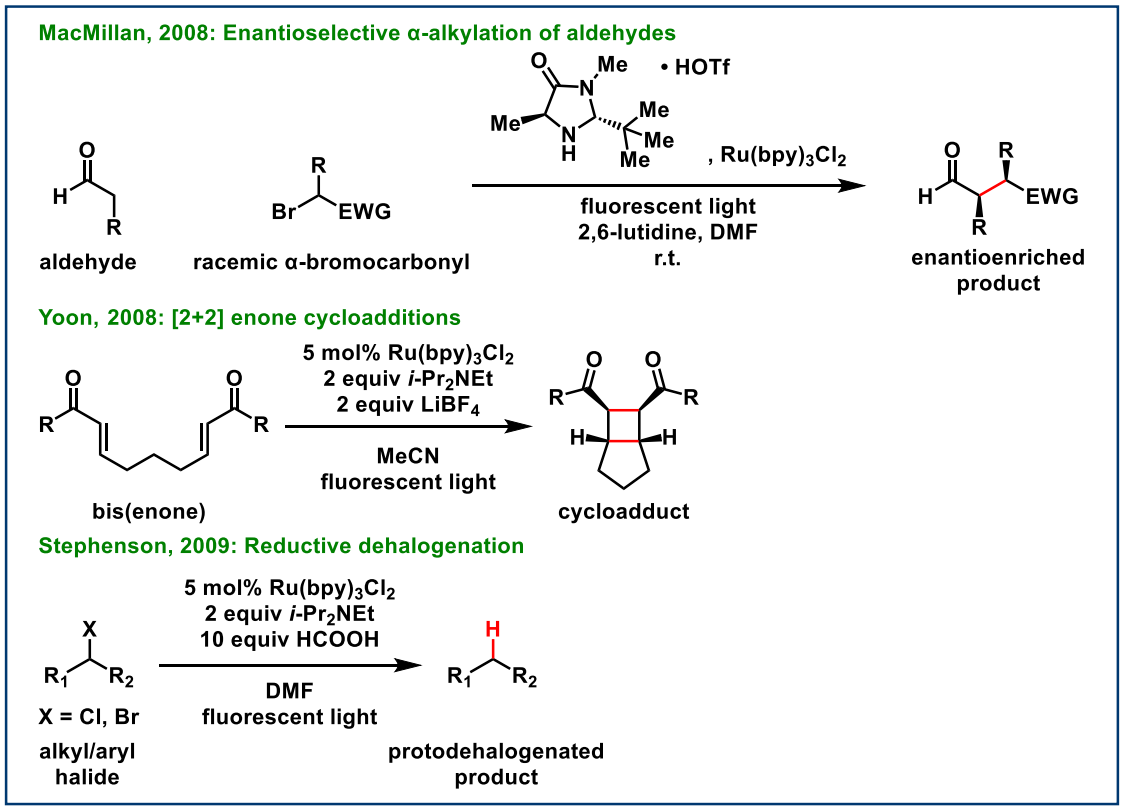

Figure 2. First reports of photoredox catalysis in synthetic methodology development.

These initial reports serve to highlight advantages of visible light photoredox reaction manifolds: the avoidance of harsh reaction conditions enable tolerance of easily oxidized or reduced moieties (e.g., alkenes, esters, arenes, silyl ethers, and carbamates), while also being environmentally benign.[23–25] Not only this, but the MacMillan group's merging of photoredox

catalysis with organocatalysis showcased the potential of dual or multi-catalytic systems, involving photocatalysts in conjunction with covalent, non-covalent, hydrogen atom transfer, and transition metal catalysis.[5,24]

1.3 Shiny Acids: Photoredox-Catalyzed Carboxylation

"Is it a blue LED or a white LED with a blue filter?"

—C. A. Sanchez

In recent years, the power of photoredox catalysis has been brought to bear in efforts to generate carboxylic acids. Carboxylic acids are desirable for several reasons; not only are they one of the most prevalent structural motifs in pharmaceutically and biologically relevant molecules, but they are also a highly desirable and synthetically valuable lynchpin enabling a wide variety of transformations.[26–28] Often, the carboxylic acid is constructed via (a) oxidation of aldehydes/primary alcohols, (b) hydrolysis of amides, esters, and nitriles, or (c) addition of organometallic species into CO_2. While these methods are versatile and are frequently used in organic synthesis, the catalytic conversion of organic (pseudo)halides to carboxylic acids has been recognized as complementary to the classical methods.[29]

The groups of Martin and Iwasawa have disclosed several methods for achieving this catalytic conversion. Initial reports utilized carbon dioxide as a carboxylate source and leveraged insertion of a metal-alkyl/aryl species into the weak CO_2 electrophile, followed by Zn/Mn reduction to turn over the catalytic Pd/Ni species (**Figure 3A**). Follow up work explored carboxylation under a metallophotoredox system, which improved upon the environmental effects by transitioning away from the usage of excess metal reductants. However, this method requires the usage of additives like Cs_2CO_3 as base (**Figure 3B**). The scope of these reactions

was thus expanded to include both aryl and alkenyl triflates as pseudohalides, and eliminate the need for additives (**Figure 3C**).[30–33]

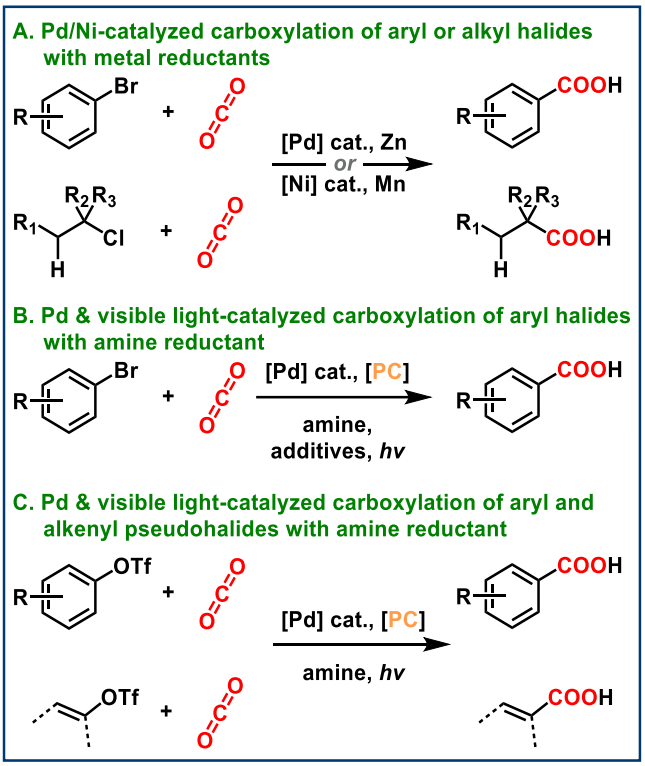

Figure 3. Previously reported methods for carboxylating aryl (pseudo)halides.

While these advances are impressive, our group felt that there would be room for further development. Recently, the Jui group reported a protocol for accessing the radical anion of carbon dioxide ($CO_2^{\bullet-}$) via a polarity matched hydrogen atom transfer (HAT) between an electrophilic thiyl radical and a formate salt. In addition, the nucleophilic and reductive reactivity of the radical anion was evaluated.[34] Inspired by this and pioneering work by Molander et al. in dual photoredox/transition metal catalysis, we imagined that reactivity of the $CO_2^{\bullet-}$ could be expanded by binding it to a metal center, allowing it to act as a one-carbon building block in catalytic cross-coupling reactions to yield carboxylates.[35]

This report will thus focus on the development of the aforementioned reactivity, enabling the construction of a wide variety of carboxylic acids bearing diverse functional groups under mild conditions from (hetero)aryl or vinyl C(sp^2)-bromide starting materials.

Chapter 2: Development of a Novel Carboxylation Method

2.1 Initial Foray into Non-Photocatalysis Land

"Ph.Ds. are made at the bench."

—A. R. LeBlanc

At the onset of this study, my mentor Gavin imagined that $CO_2^{\bullet-}$ could act as both a reductant and nucleophilic cross-coupling, partner proposing the following catalytic cycle as a potential reactive pathway (**Scheme 2**, top).

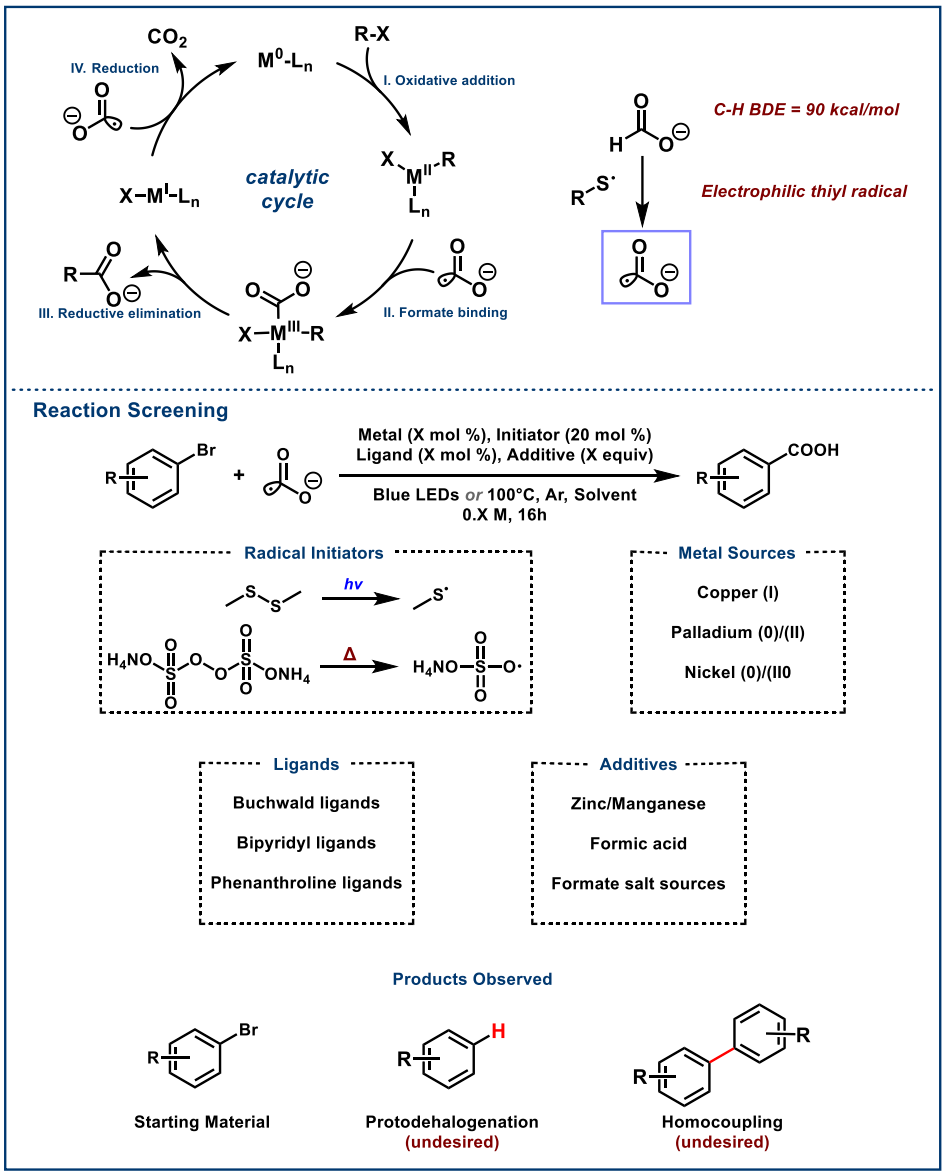

Scheme 2. (Top) Initial design and proposed catalytic cycle. (Bottom) Various reaction conditions and reagents screened, with primarily undesired products or starting material observed.

However, after in-depth screening of various catalysts, ligands, and radical initiators (for HAT), it was found that the reaction consistently returned protodehalogenated products, homocoupled products, or just starting material (**Scheme 2**, bottom). Though discouraging, Gavin hypothesized that perhaps the proposed system placed too much responsibility on $CO_2^{\bullet-}$ to both act as a nucleophile *and* reduce our metal center to regenerate the catalytic species; perhaps an additional active species whose role was to reduce the metal center would enable more efficient turnover of the catalyst. This is where I joined the project, adding considerably more to Gavin's workload by making him mentor me.

2.2 Hopping on the Photoredox Catalysis Train

"I can't change the direction of the wind, but I can adjust my sails to always reach my destination."

—Jimmy Dean

With this new hypothesis, Gavin and I turned to the use of visible light photoredox catalysis. We rationalized that not only would the excited state of a photocatalyst be capable of oxidizing an HAT agent to activate it, but it would also be able to expel an electron to reduce the transition metal center, turning over itself and the transition metal species catalytically. Thus, this kind of reactivity would leverage three intertwined catalytic cycles: a photocatalyst, transition metal, and HAT agent.

To begin our exploration here, we decided to utilize a nickel catalyst, given strong literature precedent that indicated nickel was competent in single-electron processes.[35–37] Following the Jui lab's precedent in HAT from formate using a thiol as the HAT agent, we elected to also begin by using thiols, with sodium formate as the formate source.[34] 4CzIPN was selected as the photocatalyst due to its accessibility compared to other photocatalysts; the synthesis is operationally simple (essentially a dump and stir) and utilizes cheap starting

materials, accompanied by easy purification, making it especially attractive when compared to the prices of iridium and ruthenium photocatalysts (**Scheme 3**).[38]

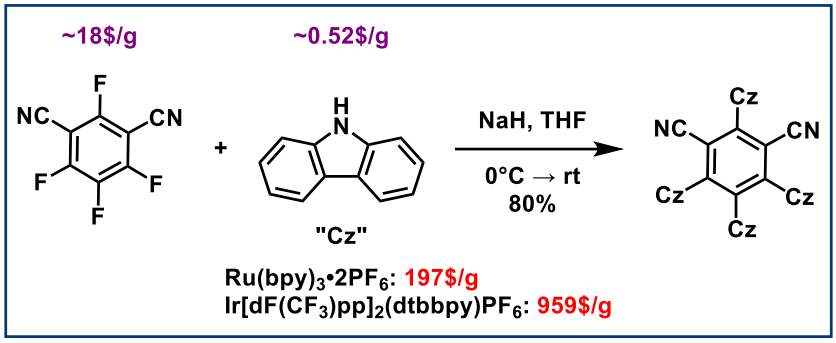

Scheme 3. Synthesis of 4CzIPN and price comparison with other common photocatalysts.

With this system as our starting point, we set out to achieve the desired transformation on 0.1 mmol scale of our model substrate, 4-bromobenzonitrile (an electron-deficient arene), through a screen of different thiol sources to identify an optimal HAT agent (**Table 1**).

Table 1. Initial HAT catalyst screen on electron-deficient arenes. Yields determined via ^{1}H NMR using CH_2Br_2 as an internal standard.

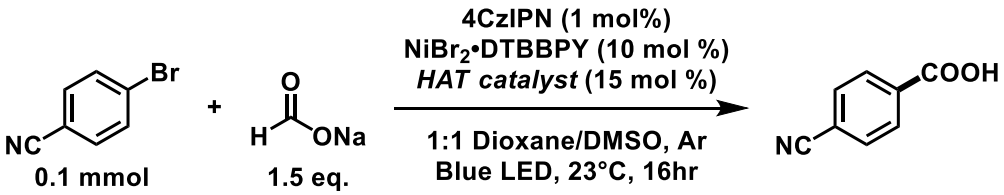

Entry	HAT Catalyst	Yield
1	Cyclohexanethiol	75%
2	Mesna	30%
3	Thiophenol	73%
4	Tert-butylthiol	51%
5	Thioacetic Acid	57%

Excitingly, we found that 4-bromobenzonitrile could be carboxylated in moderate to good yields in the conditions described by **Table 1**, with cyclohexanethiol (entry 1) as HAT catalyst furnishing the highest yield of the desired product. However, this initial hit did not translate well to other substrates. Specifically, electron-rich arenes (3-bromoanisole was used as the model

electron-rich substrate) were unable to be carboxylated, indicating potential kinetic mismatches between the desired organometallic processes and $CO_2^{\bullet-}$ formation (**Table 2**, entry 1).

Table 2. HAT catalyst screen for electron-rich arenes. Yields determined via ^{1}H NMR using CH_2Br_2 as an internal standard.

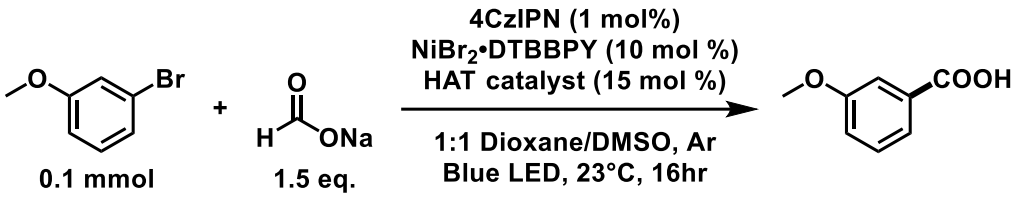

Entry	HAT Catalyst	Yield
1	CySH	0%
2	Tritylthiol	0%
3	Triisopropylsilanethiol	0%
4	DABCO	0%
5	HOBt	0%
6	NHPI	0%
7	$PhN(SO_2CF_3)_2$	98%

Both 4CzIPN ($E_{1/2}[PC^{\bullet+}/PC^*]$ = -1.2 V vs SCE) and $CO_2^{\bullet-}$ ($E_{1/2}^o$ = -2.2 V vs SCE) are competent reducing agents for generating the active nickel(0) species ($E_{1/2}^{red}[Ni^{II}/Ni^0]$ = -1.2 V vs SCE).[34,39,40] This activity may cause accumulation of Ni(0), which may then undergo catalyst deactivation pathways given the sluggish rate of oxidative addition into electron-rich/neutral aryl halides when compared to electron-deficient aryl halides.[41–43] It is also possible that the thiol HAT agent could also play a role catalyst deactivation; the Lewis basicity of thiol could lead to a tendency to coordinate the nickel metal center and poison the catalyst.[44–46] As such, a variety of different HAT agents were screened (**Table 2**). Hoping to negate potential coordination to the metal, sterically hindered thiols were examined and found to be unproductive in the system (**Table 2**, entries 2-3), as were alternative electrophilic HAT catalysts (**Table 2**, entries 4-6). We hypothesized that unorthodox HAT agents may provide a solution to this challenging problem,

and thus we examined the use of phenyl triflimide (**1**), commonly used to trap enolates as triflates. We expected that oxidation of this species would yield an electrophilic *N*-centered radical, or that reduction would result in rapid radical anion fragmentation to the nitrogenous anion (**2**) and the electrophilic sulfinyl radical (**3**) (**Figure 4A,** top).

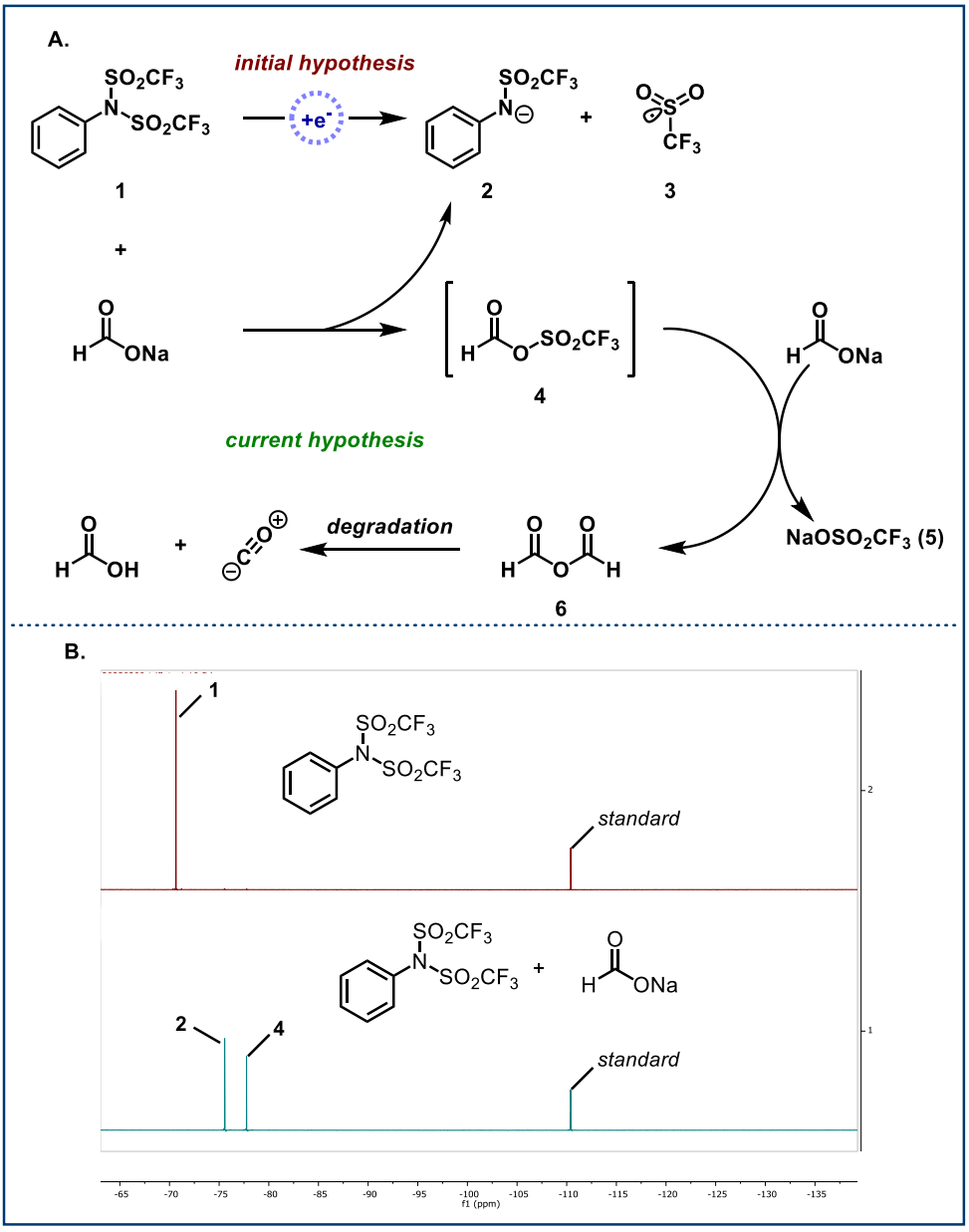

Figure 4. (A) Initial and current hypotheses for pathways towards productive HAT agents from phenyl triflimide and formate. (B) ^{19}F NMR spectra for phenyl triflimide with and without formate, demonstrating degradation of phenyl triflimide.

Gratifyingly, 15 mol % of this reagent furnished the carboxylated product of 3-bromoanisole in almost quantitative yield, leading us to question the specific activity of this species (**Table 2**, entry 7).

Cyclic voltammetry of the standard reduction potential of the phenyl triflimide indicated an irreversible reduction potential of $E_{p/2}$ = -0.90 V vs SCE (see *Supporting Information*). This indicated to us that a single-electron transfer between 4CzIPN ($E_{1/2}[PC^{\bullet+}/PC^*]$ = -1.2 V vs SCE) and phenyl triflimide is favorable, resulting in the reduction of the species. Hoping to confirm this action, ^{19}F NMR's were taken of phenyl triflimide with and without formate; intriguingly, the ^{19}F NMR instead revealed that with formate in solution, phenyl triflimide (**1**) degrades to trifluoro-*N*-phenylmethanesulfonamide (**2**) and sodium trifluoromethanesulfonate (**5**) (**Figure 4B**) (*see Supporting Information*). Though this cannot rule out the formation of a sulfinyl radical, it led us to consider other potential pathways.

Complete consumption of phenyl triflimide is observed when formate is present; given the highly electrophilic character of the species, it may react with formate to generate **4**, which is also highly electrophilic. This can react with another equivalent of formate, leading to formic anhydride (**6**) and **5** (**Figure 4A**, bottom). Control experiments using **2** and **5** revealed no product formation, indicating that they were incapable of acting as the HAT agent (**Table 3**, entries 2-3). As such, we hypothesize that it is sub-stoichiometric amounts of a reagent produced from the interaction between formate and phenyl triflimide that is responsible for HAT catalysis in the reaction system. Replacing phenyl triflimide with either methanesulfonyl chloride or *p*-toluenesulfonyl chloride—whose reactivity is analogous to phenyl triflimide—resulted in good to high yields, providing some amount of support for our hypothesis (**Table 3**, entries 4-5). However, the specific reactive HAT agent remains to be identified, and mechanistic elucidation

eludes us. Further studies must be done in order to elaborate on the complexity of this reaction mechanism. We currently propose the following set of catalytic cycles as a potential operative pathway, leaving the HAT catalytic cycle vague given the reports above (**Figure 5**).

Table 3. HAT control experiments to provide support for hypothesized mechanism. Yields determined via ^{1}H NMR using CH_2Br_2 as an internal standard.

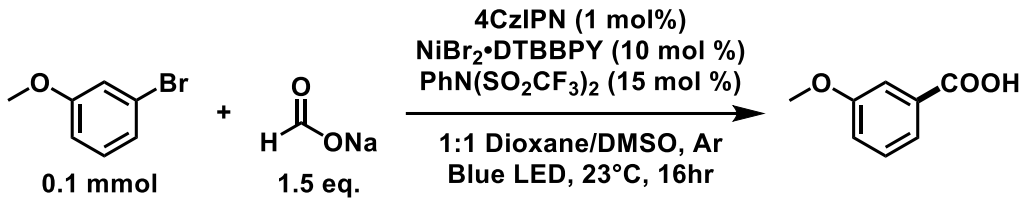

Entry	Deviation from $PhN(SO_2CF_3)_2$	Yield
1	None	98%
2	Trifluoro-*N*-Phenylmethanesulfonamide	0%
3	Trifluoromethanesulfonate	0%
4	Methanesulfonyl Chloride	90%
5	*p*-Toluenesulfonyl Chloride	76%

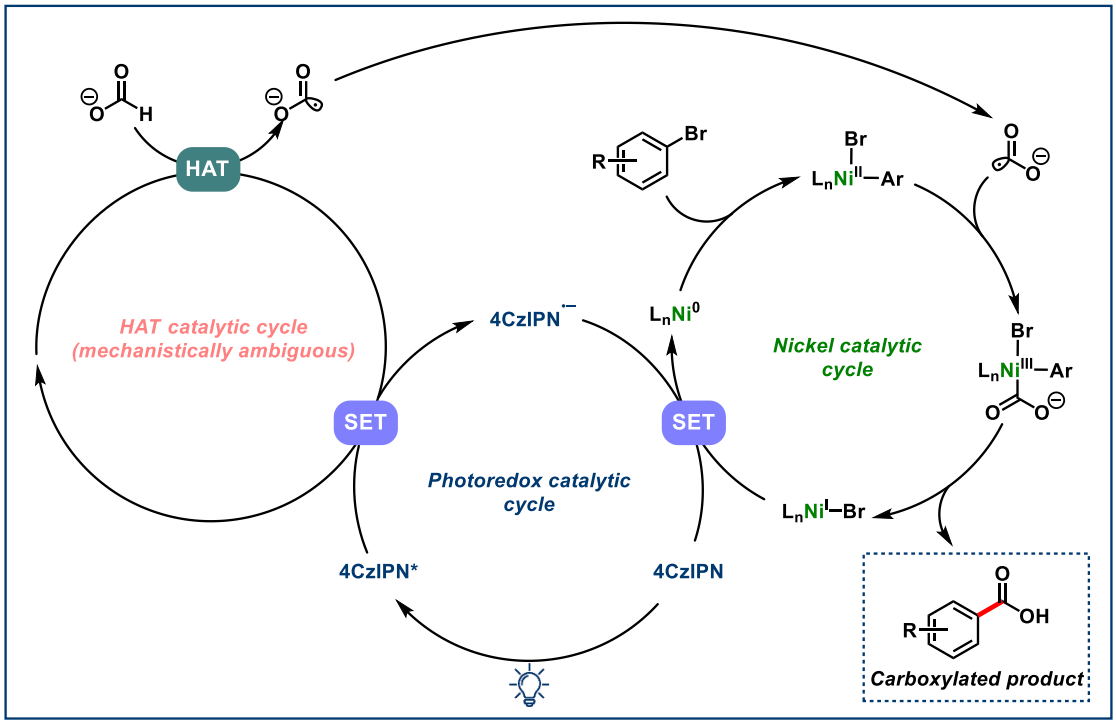

Figure 5. Proposed mechanistic pathways for the metallophotoredox/HAT catalytic cycles, with the specific HAT agent unknown.

A final solvent screen with our effective HAT catalyst in hand revealed that the initial conditions of 1:1 mixture of Dioxane:DMSO continue to be optimal for our reaction (**Table 4**, entry 1).

Table 4. Solvent optimized screen for electron-rich arenes with phenyl triflimide as the new HAT agent.

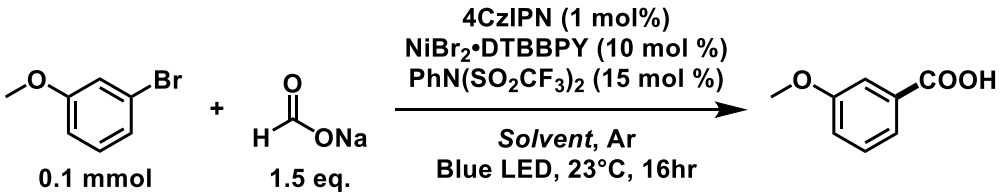

Entry	Solvent	Yield
1	1:1 Dioxane:DMSO	98%
2	Dioxane	0%
3	DMSO	85%
4	DMF	34%

In addition to this, control experiments were conducted, revealing that 4CzIPN, phenyl triflimide, formate salt, and blue LED light were all essential for carboxylation to occur, with products completely undetected in the absence of each. Unexpectedly, carboxylation occurred under ambient atmosphere when no air-free precautions were taken, albeit with a drop in yield, indicating that the reactive system may be less sensitive than anticipated (**Table 5**).

Table 5. Control experiments.

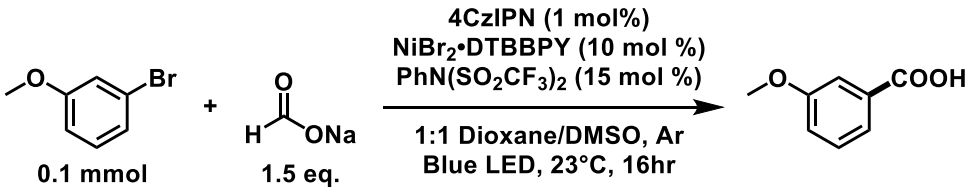

Entry	Deviation	Yield
1	No 4CzIPN	0%
2	No $PhN(SO_2CF_3)_2$	0%
3	No $NaHCO_2$	0%
4	No light	0%
5	No air-free precautions	60%

With our optimized conditions now in hand, we set out to identify the hetero(aryl) substrates amenable to carboxylation under our reaction manifold (**Table 6**). Neutral and electron-rich aryl bromides were found to undergo carboxylation in good yield (**7-12**, 51-91%), as well as electron-deficient aryl bromides (**13-20**, 76-98%). Substituents were well tolerated at the *meta* and *para* positions, but not at the *ortho* position, presumably due to steric issues around the metal center. Examples of *ortho*-substituted arenes that were poor substrates in this system include 2-bromotoluene and 2-bromobenzonitrile.

Table 6. Substrate scope of metallophotoredox-catalyzed carboxylation with formate. Isolated yields are reported unless stated otherwise. [a] Reaction performed on 0.1 mmol scale, yields determined by ^{1}H NMR using CH_2Br_2 as an internal standard.

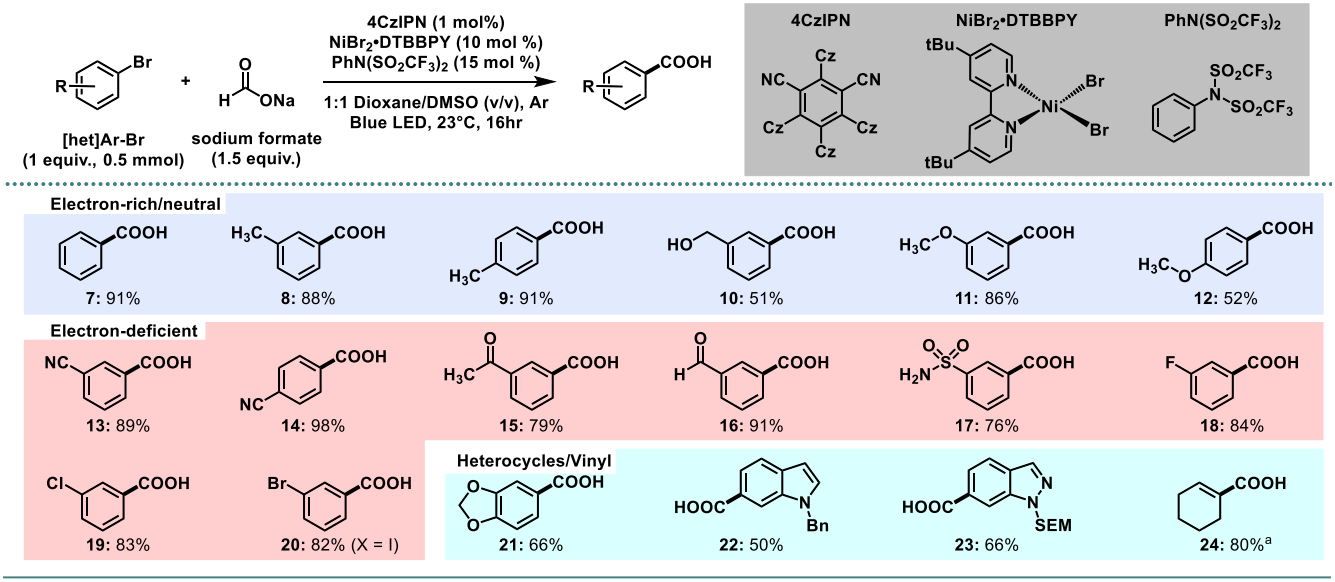

A number of functional groups including primary alcohols, ketones, aldehydes, and sulfonamides were tolerated, highlighting the mild nature of the reported carboxylation. As testament to this, neither of the carbonyl groups in **15** and **16** showed reduction to the benzylic alcohol despite being in range of reduction by $CO_2^{\bullet-}$.[47] This indicates preferential binding of $CO_2^{\bullet-}$ to the nickel catalyst over single-electron transfer to the benzylic carbonyl groups. In addition, despite the formyl C-H bond in **19** being labile with a similar BDE to formate, there is no indication of ketone formation from the acyl radical derived from the aldehyde.[40] Halogens

were also tolerated, and preferential reactivity at the C-I bond over the C-Br bond was demonstrated. Excitingly, a variety of heterocycles such as dioxolane, indole, and indazole smoothly underwent carboxylation in moderate yields (**21-23,** 50-66%), and we report cyclohexene bromide as a representative vinyl C(sp^2) bromide which was easily carboxylated in good yield (**24**). Interestingly, scale up and isolation of the carboxylated vinyl bromide proved more challenging than anticipated; though NMR yields could be determined, isolation at the 0.5 mmol scale failed in our hands.

Chapter 3: The Finale

"No quote from me would be appropriate for an honors thesis."

—G.C. Smith

To summarize this report; we have developed an effective protocol for the carboxylation of C(sp^2) bromides, which utilizes sodium formate salts as the CO_2 source. A distinct advantage that utilizing formate has over previously reported methods is that it obviates the need for gaseous reagents, simplifying reaction setup and reducing synthetic effort, due to the crystalline and bench-stable nature of sodium formate. In addition, usage of phenyl triflimide enables *in situ* generation of an active HAT agent; leveraging phenyl triflimide in this way is poorly precedented in the literature, though it appears to enable abstraction of the formyl hydrogen in formate and is potentially underutilized as an HAT agent. Further mechanistic studies must be undertaken in order to better understand the specific role of phenyl triflimide and identify the particular species responsible for HAT activity, shining a light on the complex nature of the reaction mechanism. Overall, we have demonstrated the successful carboxylation of electronically distinct hetero(aryl)/vinyl bromides under mild catalytic conditions, achieving our initial goal with some intriguing tidbits for further research.

Supporting Information

I. General Information

General Reagent Information

Reagents were purchased from Sigma-Aldrich, Alfa Aesar, Acros Organics, Combi-Blocks, Oakwood Chemicals, Astatech, and TCI America and used as received, unless stated otherwise. All reactions were set up on the bench top and conducted under argon atmosphere while subject to irradiation from blue LEDs (LEDwholesalers PAR38 Indoor Outdoor 16-Watt LED Flood Light Bulb, Blue; or Hydrofarm® PPB1002 PowerPAR LED Bulb-Blue 15W/E27 (available from Amazon). Flash chromatography was carried out using Siliaflash® P60 silica gel obtained from Silicycle. Thin-layer chromatography (TLC) was performed on 250 µm SiliCycle silica gel F-254 plates. Visualization of the developed chromatogram was performed by fluorescence quenching or staining using $KMnO_4$, p-anisaldehyde, or ninhydrin stains. DMSO was purchased from Fisher Scientific and was distilled over CaH_2 and degassed by sonication under vacuum and stored under nitrogen. Photoredox catalyst 4CzIPN was prepared according to literature procedures.

General Analytical Information

Unless otherwise noted, all yields refer to chromatographically and spectroscopically (^{1}H NMR) homogenous materials. New compounds were characterized by NMR and HRMS. ^{1}H and ^{13}C NMR spectra were obtained from the Emory University NMR facility and recorded on a Bruker Avance III HD 600 equipped with cryo-probe (600 MHz), Bruker 400 (400 MHz), INOVA 600 (600 MHz), INOVA 500 (500 MHz), INOVA 400 (400 MHz), or VNMR 400 (400 MHz), and are internally referenced to residual solvent signals. Data for 1H NMR are reported as follows: chemical shift (ppm), multiplicity (s = singlet, d = doublet, t = triplet, q = quartet, m = multiplet, dd = doublet of doublets, dt = doublet of triplets, ddd= doublet of doublet of doublets, dtd= doublet of triplet of doublets, b = broad, etc.), coupling constant (Hz), integration, and assignment, when applicable. Data for decoupled ^{13}C NMR are reported in terms of chemical shift and multiplicity when applicable. High Resolution mass spectra were obtained from the Emory University Mass Spectral facility.

Abbreviations

DMSO = dimethyl sulfoxide

DMF = dimethylformamide

THF = tetrahydrofuran

DCM = dichloromethane

TLC = thin layer chromatograph

TEA = triethylamine

EtOAc = ethyl acetate

MeCN = acetonitrile

LCMS = liquid chromatography mass spectrometry

GCMS = gas chromatography mass spectrometry

MeOH = methanol

General Photoredox Reaction Setup

To run multiple reactions, an appropriately sized 3D printed carousel was used, which exposed the reactions to the blue light evenly (photo 1). A 15 W LED array lamp was used as a blue light source (photo 2,3). These lamps were routinely used for up to 12 reactions at a time (photo 2,3). The blue LEDs were positioned approximately 6 inches above the reaction vials for good light coverage without overheating the reactions (photo 2,3).

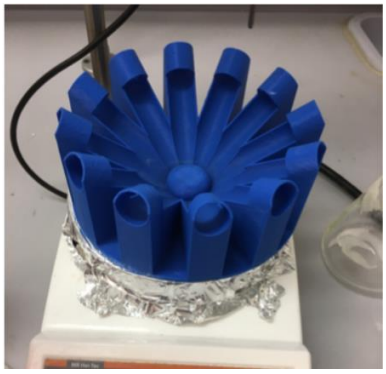

Photo 1

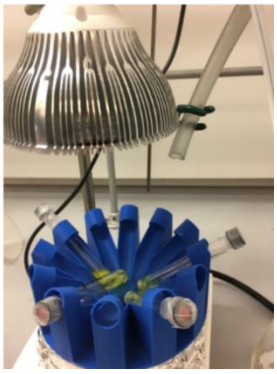

Photo 2

Photo 3

II. General Procedures
General Procedure for Photoredox Reactions:

A 20 mL screw-top test tube was charged with 4CzIPN (1 mol%), sodium formate (1.5 equiv), mesna (20 mol%), N-phenyl-bis(trifluoromethanesulfonimide) (15 mol%) and [4,4'-Bis(1,1-dimethyl)-2,2'-bipyridine] nickel (II) bromide (10 mol%)) and substrate (1 equiv., if solid). The tube was equipped with a stir bar and was sealed with a PTFE/silicon septum. The atmosphere was exchanged by applying vacuum and backfilling with argon (this process was conducted a total of three times). Under argon atmosphere, the indicated degassed solvent (0.1 M) was added via syringe followed by the substrate (if liquid, 1.0 equiv). The resulting mixture was stirred at 1400 RPM for 16 h under irradiation by blue LEDs. 1M HCl was added and then the reaction mixture was extracted with ethyl acetate (3 x). The organic layer was dried over $MgSO_4$ and concentrated. The residue was purified on silica using the indicated solvent mixture as eluent to afford the title compound.

III. Electrochemical Measurements & ^{19}F Spectra

Electrochemical potentials were obtained with a standard set of conditions according to literature procedure.[47] Cyclic voltammograms (CVs) were collected with a VersaSTAT 4Potentiostat. Samples were prepared with 0.1 mmol of substrate in 10 mL of 0.1 M tetra-n-butylammonium hexafluorophosphate in dry, degassed acetonitrile. Measurements employed a glassy carbon working electrode, platinum wire counter electrode, 3M NaCl silver-silver chloride reference electrode, and a scan rate of 100 mV/s. Reductions were measured by scanning potentials in the negative direction and oxidations in the positive direction; the glassy carbon electrode was polished between each scan. Data was analyzed using Microsoft Excel by subtracting a background current prior to identifying the maximum current (Cp) and determining the potential (Ep/2) at half this value (Cp/2). The obtained value was referenced to Ag|AgCl and converted to SCE by subtracting 0.035 V.

Cyclic Voltammogram for Phenyl Triflimide

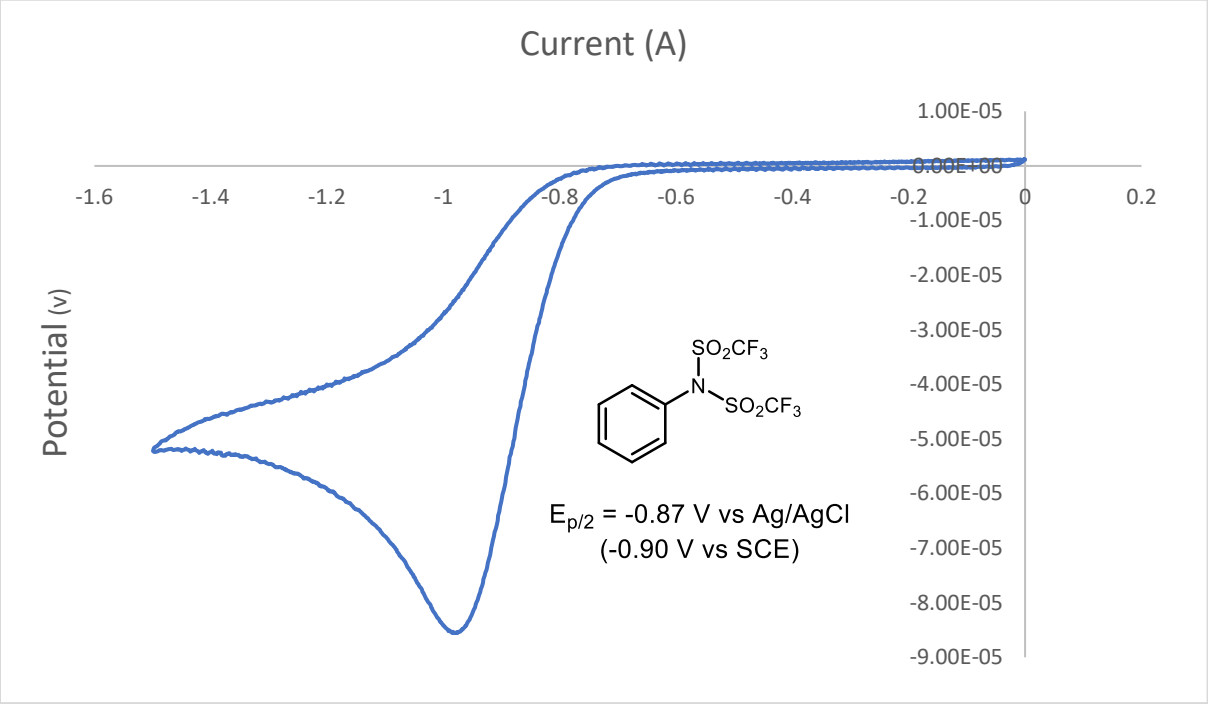

^{19}F Spectra of Phenyl Triflimide, Sodium Formate + Phenyl Triflimide

Samples were prepared using 0.015 mmol of phenyl triflimide (**A**) alongside a combination of 0.015 mmol phenyl triflimide and 0.15 mmol sodium formate (**B**) using 1-bromo-3-fluorobenzene as an internal standard.

Spectra **B** shows trifluoro-*N*-phenylmethanesulfonamide at -75.56 ppm, alongside sodium trifluoromethanesulfonate at -77.76 ppm. These chemical shifts are consistent with previously reported literature spectra.[48]

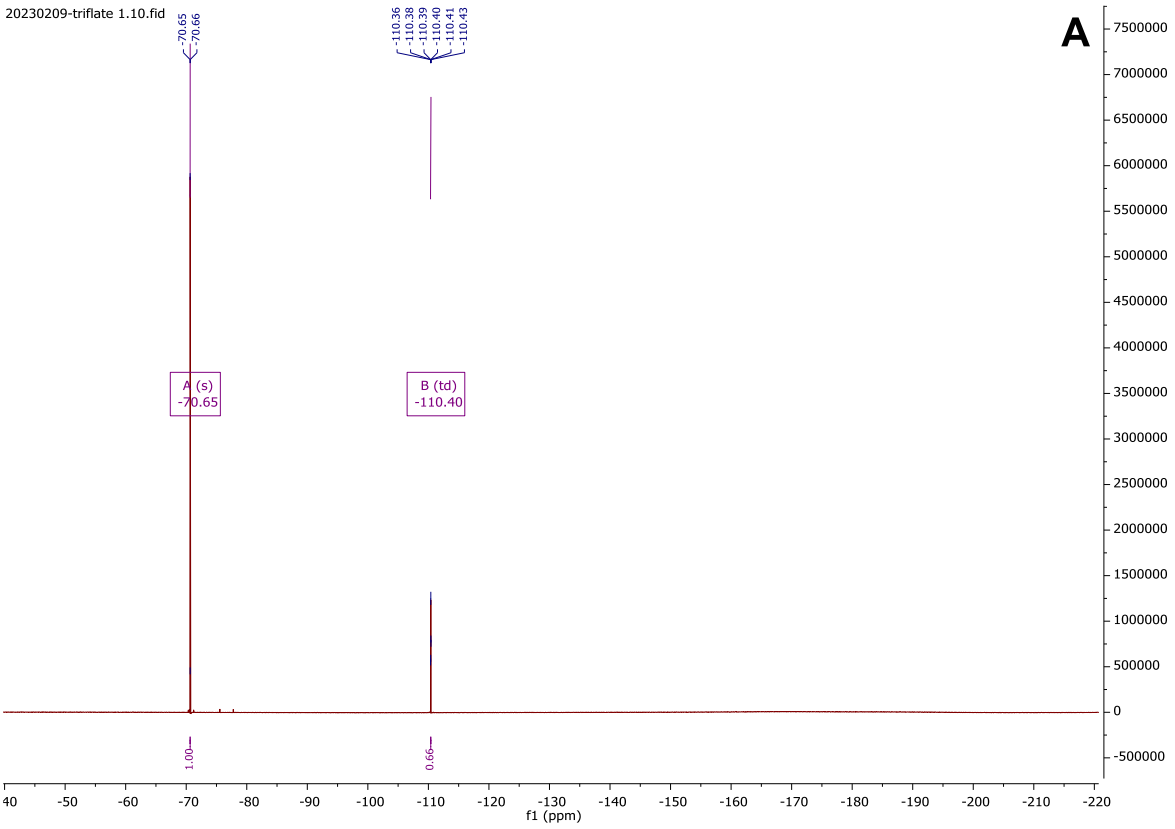
20230209-triflate 1.10.fid
A
-70.65
-70.66
-110.36
-110.38
-110.39
-110.40
-110.41
-110.43
A (s)
-70.65
B (td)
-110.40
1.00
0.66
f1 (ppm)

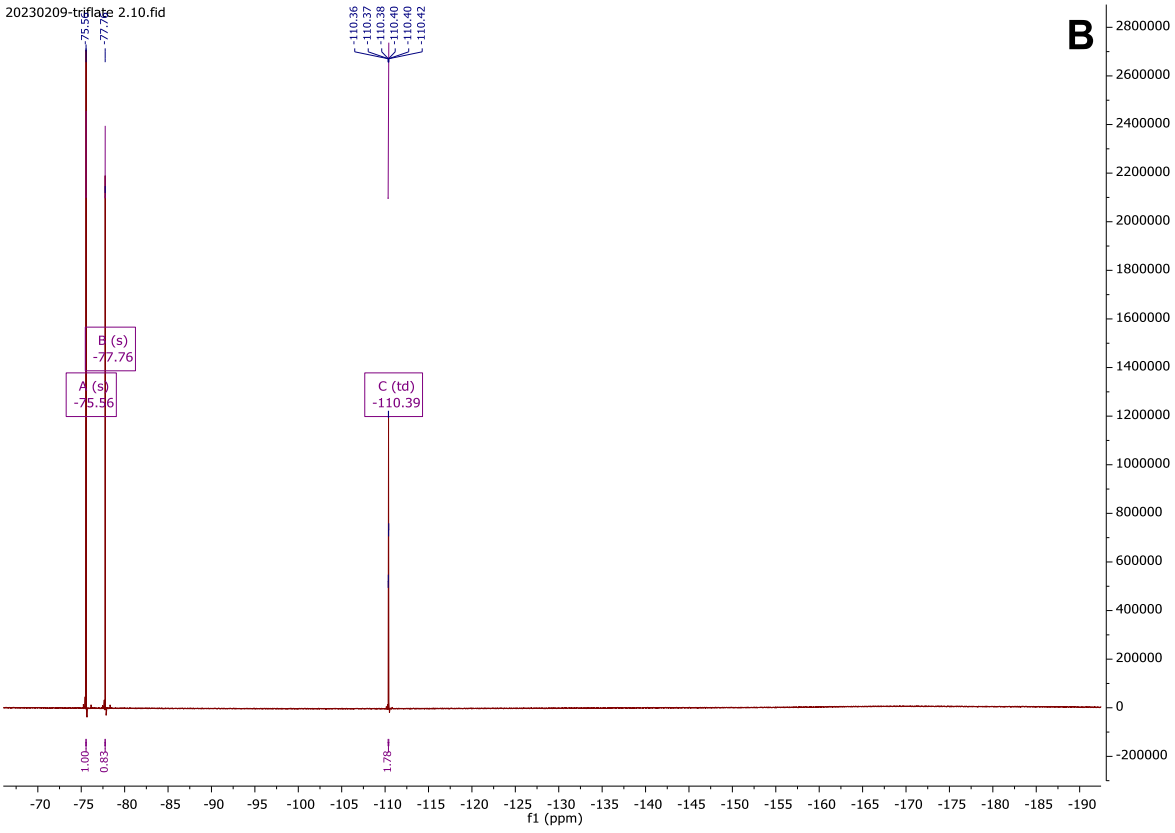
20230209-triflate 2.10.fid
B
-75.56
-77.76
-110.36
-110.37
-110.38
-110.40
-110.42
B (s)
-77.76
A (s)
-75.56
C (td)
-110.39
1.00
0.83
1.78
f1 (ppm)

III. Preparation of Starting Materials

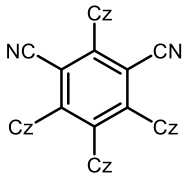

2,4,5,6-Tetrakis(carbazole-9-yl)-4,6-dicyanobenzene (4CzIPN) (S1): To a flame dried round bottom flask was added carbazole (1.67 g, 10.0 mmol) in anhydrous THF (40 mL). Sodium hydride (60% in oil, 0.60 g, 15.0 mmol) was carefully added portion wise to the solution. After 30 minutes, tetrafluoroisopthalonitrile (0.40 g, 2.00 mmol) was added and allow to stir at room temperature for 16 h. Water (2 mL) was then added carefully, and the reaction mixture was then concentrated in vacuo. The resulting solid was then washed with water and ethanol then recrystallized from hexanes/DCM to yield the product as a vibrant yellow solid (1.4 g, 89% yield). The physical and spectral properties were consistent with reported values.[39]

^{1}H NMR (400 MHz, $CDCl_3$): δ 8.21 (d, J = 7.8 Hz, 1H), 7.49 (t, J = 7.9 Hz, 2H), 7.33 (d, J = 7.5 Hz, 2H), 7.24-7.19 (m, 4H), 7.14-7.20 (m, 8H), 6.83 (t, J = 7.8 Hz, 4H), 6.63 (t, J = 7.6 Hz, 2H).

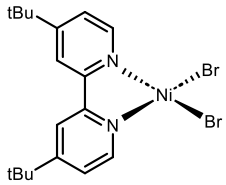

[4,4'-Bis(1,1-dimethyl)-2,2'-bipyridine] nickel (II) bromide (S2): Following a previously reported synthesis, a flame-dried round bottom flask was charged with $NiBr_2$(glyme) (0.616 g, 2.0 mmol, 1 equiv.) and 4,4'-di-tert¬-butyl-2,2'-bipyridyl (0.536 g, 2.0 mmol, 1 equiv.) before being placed under argon. Anhydrous THF (60 mL) was added, and the reaction mixture was stirred for 20 h. The resulting green solid was filtered off and washed with diethyl ether to afford the title compound as a green solid that was used without further purification.

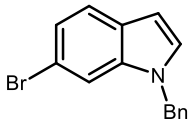

1-benzyl-6-bromo-1H-indole (S3): To a flame-dried round bottom flask was added 6-bromoindole (0.98 g, 5.0 mmol, 1 equiv.) followed by anhydrous DMF (5 mL). The reaction mixture was cooled to 0°C and sodium hydride (0.24 g, 6.0 mmol, 1.2 equiv.) was added portion wise. The mixture was stirred for thirty minutes at 0°C and then benzyl bromide (0.9 mL, 7.5 mmol, 1.5 equiv., dissolved in 2.5 mL DMF) was added slowly. The reaction mixture was allowed to warm to room temperature and stirred overnight. After cooling back down to 0°C, the reaction was quenched with water (5 mL), extracted three times with ethyl acetate, dried over $MgSO_4$ and concentrated in vacuo. The crude reaction mixture was then purified by silica chromatography (2.5 % EtOAc/Hexanes as the eluent) to afford the title compound as an off white solid (1.08 g, 76% yield).[49]

^{1}H NMR (400 MHz, $CDCl_3$): δ 7.50 (d, J = 8.4 Hz, 1H), 7.45-7.41 (m, 1H), 7.36-7.27 (m, 3H), 7.21 (dd, J = 8.4 Hz, 1.7 Hz, 1H), 7.12-7.03 (m, 3H), 6.52 (dd, J = 3.1, 1.0 Hz, 1H), 5. 28 (s, 2H).

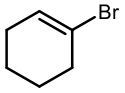

1-bromocylcohex-1-ene (S4): To a flame-dried round bottom flask was added triphenyl phosphite (6.8 g, 22.0 mmol, 1.1 equiv.). The atmosphere was exchanged three times with argon and equipped with an argon balloon. Anhydrous CH_2Cl_2 was added (60 mL) and the reaction was cooled to -78°C. Bromine (1.2 mL, 24.0 mmol, 1.2 equiv.) was added slowly and allowed to stir for five minutes before the slow addition of triethylamine (3.6 mL, 26.0 mmol, 1.3 equiv.). The reaction mixture was stirred for another five minutes before the addition of cyclohexanone (2.1 mL, 20.0 mmol, 1 equiv.). The reaction mixture was warmed to room temperature overnight then refluxed for two hours. The crude reaction mixture was then concentrated and purified by silica chromatography (100% Hexanes as the eluent) to afford the title compound as a pale-yellow oil (1.83 g, 56% yield). The physical and spectral properties match the reported values.[50]

^{1}H NMR (400 MHz, $CDCl_3$): δ 6.04 (m, 1H), 2.42 (m, 2H), 2.08-2.07 (m, 2H)), 1.77-1.71 (m, 2H), 1.64-1.58 (m, 2H).

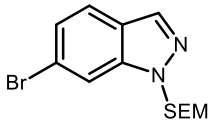

6-bromo-1-((2-(trimethylsilyl)ethoxy)methyl)-1H-indazole (S5): To a round bottom flask was added 6-bromoindazole (0.493 g, 2.5 mmol, 1 equiv.) and CH2Cl2 (10 mL). The reaction mixture was cooled to 0°C and potassium hydroxide (0.168 g, 3.0 mmol, 3 equiv., dissolved in 0.6 mL H2O) was added, followed by tetrabutylammonium bromide (0.080 g, 0.25 mmol, 0.1 equiv.). SEM-chloride (0.49 mL, 2.75 mmol, 1.1 equiv.) was then added dropwise and stirred at 0°C for 1 hour. The reaction mixture was allowed to warm to room temperature, stirred overnight, quenched with H_20 (10 mL) and extracted three times with DCM. The crude reaction mixture was dried over $MgSO_4$, concentrated in vacuo, and purified via silica chromatography (5-10% EtOAc/Hexanes as the eluent) to afford the title compound as a light brown oil (0.412 g, 50% yield).

^{1}H NMR (400 MHz, $CDCl_3$): δ 7.97 (d, J = 1.0 Hz, 1H), 7.79-7.77 (m, 1H), 7.60 (dd, J = 8.6 Hz, 0.7 Hz, 1H), 7.30 (dd, J = 8.5 Hz, 1.6 Hz, 1H), 5.70 (s, 2H), 3.56-3.50 (m, 2H), 0.91-0.85 (m, 3H), -0.06 (s, 9H).

^{13}C NMR (100 MHz, $CDCl_3$): δ 140.61, 134.24, 125.11 123.76, 122.32, 121.36, 112.92, 77.95, 66.67 17.86, -1.11 -1.36, -1.61.

HRMS (APCI) m/z: [M+] calcd. for C12H20ON2Si, 327.0523, found 327.0520.

R_f: 0.47 (5% EtOAc/Hexanes).

IV. Preparation of Products from Substrate Table

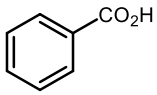

Benzoic Acid (7): Prepared according to the general procedure using bromobenzene (0.5 mmol, 53 µl, 1 equiv.), sodium formate (0.75 mmol, 0.051 g, 1.5 equiv.), 4CzIPN (.005 mmol, 0.0039 g, 1 mol%), N-phenyl-bis(trifluoromethanesulfonimide) (0.075 mmol, 0.027 g, 15 mol%), and [4,4'-Bis(1,1-dimethyl)-2,2'-bipyridine] nickel (II) bromide (0.05 mmol, 0.024 g, 10 mol%), in 1:1 DMSO/dioxane (5 mL). After 16 hours the reaction was quenched with 1M HCl (10 mL), extracted three times with ethyl acetate, dried over $MgSO_4$ and concentrated in vacuo. The crude reaction mixture was purified by silica chromatography (10% EtOAc/hexanes + 1% AcOH as the eluent) to afford the title compound as a pale-yellow solid (0.065 g, 86% yield). The physical and spectral properties were consistent with the reported values.[51]

^{1}H NMR (400 MHz, DMSO-d_6): δ 12.94 (s, 1H), 7.95 (d, J = 7.3 Hz, 2H), 7.62 (t, J = 7.3 Hz, 2H), 7.50 (t, J = 7.7 Hz, 1H).

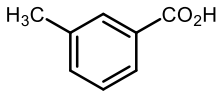

3-methylbenzoic acid (8): Prepared according to the general procedure using 3-bromotoluene (0.5 mmol, 61 µl, 1 equiv.), sodium formate (0.75 mmol, 0.051 g, 1.5 equiv.), 4CzIPN (.005 mmol, 0.0039 g, 1 mol%), N-phenyl-bis(trifluoromethanesulfonimide) (0.075 mmol, 0.027 g, 15 mol%), and [4,4'-Bis(1,1-dimethyl)-2,2'-bipyridine] nickel (II) bromide (0.05 mmol, 0.024 g, 10 mol%), in 1:1 DMSO/dioxane (5 mL). After 16 hours the reaction was quenched with 1M HCl (10 mL), extracted three times with ethyl acetate, dried over $MgSO_4$ and concentrated in vacuo. The crude reaction mixture was purified by silica chromatography (20% EtOAc/hexanes + 1% AcOH as the eluent) to afford the title compound as a pale-yellow solid (0.060 g, 88% yield). The physical and spectral properties were consistent with the reported values.[52]

^{1}H NMR (600 MHz, $CDCl_3$): δ 7.95-7.90 (m, 2H), 7.43 (d, J = 7.6z Hz, 2H), 7.38 (t, J = 7.4 Hz, 1H), 2.43 (s, 3H).

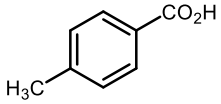

4-methylbenzoic acid (9): Prepared according to the general procedure using 4-bromotoluene (0.5 mmol, 61 µl, 1 equiv.), sodium formate (0.75 mmol, 0.051 g, 1.5 equiv.), 4CzIPN (.005 mmol, 0.0039 g, 1 mol%), N-phenyl-bis(trifluoromethanesulfonimide) (0.075 mmol, 0.027 g, 15 mol%), and [4,4'-Bis(1,1-dimethyl)-2,2'-bipyridine] nickel (II) bromide (0.05 mmol, 0.024 g, 10 mol%), in 1:1 DMSO/dioxane (5 mL). After 16 hours the reaction was quenched with 1M HCl (10 mL), extracted three times with ethyl acetate, dried over $MgSO_4$ and concentrated in vacuo. The crude reaction mixture was purified by silica chromatography (20% EtOAc/hexanes + 1% AcOH as the eluent) to afford the title compound as a pale-yellow solid (0.060 g, 88% yield). The physical and spectral properties were consistent with the reported values.[53]

^{1}H NMR (600 MHz, $CDCl_3$): δ 7.95-7.90 (m, 2H), 7.43 (d, J = 7.6z Hz, 2H), 7.38 (t, J = 7.4 Hz, 1H), 2.43 (s, 3H).

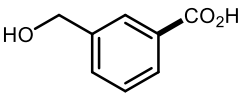

3-(hydroxymethyl)benzoic acid (10): Prepared according to the general procedure using 3-bromobenzyl alcohol (0.5 mmol, 60 µl, 1 equiv.), sodium formate (0.75 mmol, 0.051 g, 1.5 equiv.), 4CzIPN (.005 mmol, 0.0039 g, 1 mol%), N-phenyl-bis(trifluoromethanesulfonimide) (0.075 mmol, 0.027 g, 15 mol%), and [4,4'-Bis(1,1-dimethyl)-2,2'-bipyridine] nickel (II) bromide (0.05 mmol, 0.024 g, 10 mol%), in 1:1 DMSO/dioxane (5 mL). After 16 hours the reaction was quenched with 1M HCl (10 mL), extracted three times with ethyl acetate, dried over $MgSO_4$ and concentrated in vacuo. The crude reaction mixture was purified by silica chromatography (20-50% EtOAc/hexanes + 1% AcOH as the eluent) to afford the title compound as a white solid (0.039 g, 51% yield).

^{1}H NMR (400 MHz, DMSO-d_6): δ 7.92 (s, 1H), 7.81 (d, J = 7.7 Hz, 1H), 7.54 (d, J = 7.7 Hz, 1H) 7.44 (t, J = 7.6 Hz, 1H) 5.32 (bs, 1H), 4.55 (s, 2H).

^{13}C NMR (100 MHz, $CDCl_3$): δ 167.46, 143.07. 130.77, 130.68, 128.31, 127.64, 127.21, 62.44.

HRMS (APCI) m/z: [M+H] calcd. for C8H9O3, 153.0546, found 153.0546.

R_f: 0.36 (40% EtOAc/Hexanes + 1% AcOH).

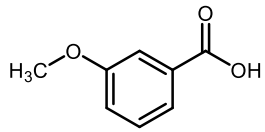

3-methoxybenzoic acid (11): Prepared according to the general procedure using 3-bromoanisole (0.5 mmol, 63 µl, 1 equiv.), sodium formate (0.75 mmol, 0.051 g, 1.5 equiv.), 4CzIPN (.005 mmol, 0.0039 g, 1 mol%), N-phenyl-bis(trifluoromethanesulfonimide) (0.075 mmol, 0.027 g, 15 mol%), and [4,4'-Bis(1,1-dimethyl)-2,2'-bipyridine] nickel (II) bromide (0.05 mmol, 0.024 g, 10 mol%), in 1:1 DMSO/dioxane (5 mL). After 16 hours the reaction was quenched with 1M HCl (10 mL), extracted three times with ethyl acetate, dried over $MgSO_4$ and concentrated in vacuo. The crude reaction mixture was purified by silica chromatography (20-30% EtOAc/hexanes + 1% AcOH as the eluent) to afford the title compound as a pale-yellow solid (0.065 g, 86% yield). The physical and spectral properties were consistent with the reported values.[54]

^{1}H NMR (400 MHz, DMSO-d_6): δ 13.00 (s, 1H), 7.53 (dt, J = 7.6, 1.3 Hz, 1H), 7.44-7.38 (m, 2H), 7.18 (ddd, J = 8.20, 2.7, 1.0 Hz, 1H), 3.80 (s, 3H).

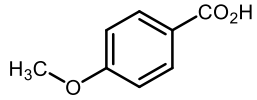

4-methoxybenzoic acid (12): Prepared according to the general procedure using 4-bromoanisole (0.5 mmol, 63 µl, 1 equiv.), sodium formate (0.75 mmol, 0.051 g, 1.5 equiv.), 4CzIPN (.005 mmol, 0.0039 g, 1 mol%), N-phenyl-bis(trifluoromethanesulfonimide) (0.075 mmol, 0.027 g, 15 mol%), and [4,4'-Bis(1,1-dimethyl)-2,2'-bipyridine] nickel (II) bromide (0.05 mmol, 0.024 g, 10

mol%), in 1:1 DMSO/dioxane (5 mL). After 16 hours the reaction was quenched with 1M HCl (10 mL), extracted three times with ethyl acetate, dried over $MgSO_4$ and concentrated in vacuo. The crude reaction mixture was purified by silica chromatography (20-30% EtOAc/hexanes + 1% AcOH as the eluent) to afford the title compound as a pale-yellow solid (0.039 g, 52% yield). The physical and spectral properties were consistent with the reported values.[54]

^{1}H NMR (400 MHz, DMSO-d_6): δ 13.00 (s, 1H), 7.89 (d, J = 7.9, 2H), 7.02 (d, J = 8.8 Hz, 2H), 3.82 (s, 3H).

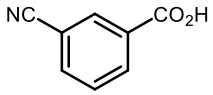

3-cyanobenzoic acid (13): Prepared according to the general procedure using 3-bromobenzonitrile (0.5 mmol, 0.091g, 1 equiv.), sodium formate (0.75 mmol, 0.051 g, 1.5 equiv.), 4CzIPN (.005 mmol, 0.0039 g, 1 mol%), N-phenyl-bis(trifluoromethanesulfonimide) (0.075 mmol, 0.027 g, 15 mol%), and [4,4'-Bis(1,1-dimethyl)-2,2'-bipyridine] nickel (II) bromide (0.05 mmol, 0.024 g, 10 mol%), in 1:1 DMSO/dioxane (5 mL). After 16 hours the reaction was quenched with 1M HCl (10 mL), extracted three times with ethyl acetate, dried over $MgSO_4$ and concentrated in vacuo. The crude reaction mixture was purified by silica chromatography (20-30% EtOAc/hexanes + 1% AcOH as the eluent) to afford the title compound as a white solid (0.062 g, 89% yield). The physical and spectral properties were consistent with the reported values.[55]

^{1}H NMR (400 MHz, DMSO-d_6): δ 13.00 (s, 1H), 8.30-8.26 (m 1H), 8.25-8.20 (dt, J = 7.9, 1.4 Hz, 1H), 8.13-8.07 (dt, J = 7.7, 1.3, 1H), 7.73 (t, J = 7.8 Hz, 1H).

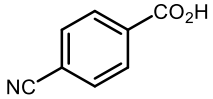

4-cyanobenzoic acid (14): Prepared according to the general procedure using 4-bromobenzonitrile (0.5 mmol, 0.091g, 1 equiv.), sodium formate (0.75 mmol, 0.051 g, 1.5 equiv.), 4CzIPN (.005 mmol, 0.0039 g, 1 mol%), N-phenyl-bis(trifluoromethanesulfonimide) (0.075 mmol, 0.027 g, 15 mol%), and [4,4'-Bis(1,1-dimethyl)-2,2'-bipyridine] nickel (II) bromide (0.05 mmol, 0.024 g, 10 mol%), in 1:1 DMSO/dioxane (5 mL). After 16 hours the reaction was quenched with 1M HCl (10 mL), extracted three times with ethyl acetate, dried over $MgSO_4$ and concentrated in vacuo. The crude reaction mixture was purified silica chromatography (20-30% EtOAc/hexanes + 1% AcOH as the eluent) to afford the title compound as a pale-yellow solid (0.065 g, 86% yield). The physical and spectral properties were consistent with the reported values.[56]

^{1}H NMR (400 MHz, $CDCl_3$): δ 8.22 (d, J = 8.4 Hz, 2H), 7.80 (d, J = 8.4 Hz, 2H).

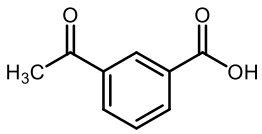

3-acetylbenzoic acid (15): Prepared according to the general procedure using 3-bromoacetophenone (0.5 mmol, 66 µl, 1 equiv.), sodium formate (0.75 mmol, 0.051 g, 1.5

equiv.), 4CzIPN (.005 mmol, 0.0039 g, 1 mol%), N-phenyl-bis(trifluoromethanesulfonimide) (0.075 mmol, 0.027 g, 15 mol%), and [4,4'-Bis(1,1-dimethyl)-2,2'-bipyridine] nickel (II) bromide (0.05 mmol, 0.024 g, 10 mol%), in 1:1 DMSO/dioxane (5 mL). After 16 hours the reaction was quenched with 1M HCl (10 mL), extracted three times with ethyl acetate, dried over $MgSO_4$ and concentrated in vacuo. The crude reaction mixture was purified by silica chromatography (20-30% EtOAc/hexanes + 1% AcOH as the eluent) to afford the title compound as a white solid (0.065 g, 79% yield). The physical and spectral properties were consistent with the reported values.[57]

^{1}H NMR (400 MHz, $CDCl_3$): δ 8.68 (s, 1H), 8.32 (d, J = 7.7 Hz, 1H), 8.23 (d, J = 7.9 Hz, 1H), 7.62 (t, J = 7.8 Hz, 1H), 2.68 (s, 3H).

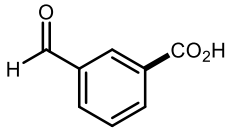

3-formylbenzoic acid (16): Prepared according to the general procedure using 3-bromobenzaldehyde (0.5 mmol, 0.093 g, 1 equiv.), sodium formate (0.75 mmol, 0.051 g, 1.5 equiv.), 4CzIPN (.005 mmol, 0.0039 g, 1 mol%), N-phenyl-bis(trifluoromethanesulfonimide) (0.075 mmol, 0.027 g, 15 mol%), and [4,4'-Bis(1,1-dimethyl)-2,2'-bipyridine] nickel (II) bromide (0.05 mmol, 0.024 g, 10 mol%), in 1:1 DMSO/dioxane (5 mL). After 16 hours the reaction was quenched with 1M HCl (10 mL), extracted three times with ethyl acetate, dried over $MgSO_4$ and concentrated in vacuo. The crude reaction mixture was purified by silica chromatography (20% EtOAc/hexanes + 1% AcOH as the eluent) to afford the title compound as a pale-yellow solid (0.068 g, 91% yield). The physical and spectral properties were consistent with the reported values.[58]

^{1}H NMR (400 MHz, DMSO-d_6): δ 13.37 (s, 1H), 10.09 (s, 1H), 8.44 (s, 1H), 8.24 (d, J = 7.6 Hz, 1H), 8.14 (d, J = 7.7 Hz, 1H), 7.74 (t, J = 7.6 Hz, 1H).

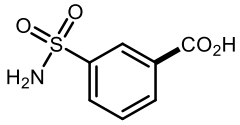

3-sulfamoylbenzoic acid (17): Prepared according to the general procedure using 3-bromobenzenesulfonamide (0.5 mmol, 0.118 g, 1 equiv.), sodium formate (0.75 mmol, 0.051 g, 1.5 equiv.), 4CzIPN (.005 mmol, 0.0039 g, 1 mol%), N-phenyl-bis(trifluoromethanesulfonimide) (0.075 mmol, 0.027 g, 15 mol%), and [4,4'-Bis(1,1-dimethyl)-2,2'-bipyridine] nickel (II) bromide (0.05 mmol, 0.024 g, 10 mol%), in 1:1 DMSO/dioxane (5 mL). After 16 hours the reaction was quenched with 1M HCl (10 mL), extracted three times with ethyl acetate, dried over $MgSO_4$ and concentrated in vacuo. The crude reaction mixture was purified by silica chromatography purified by silica chromatography (0-50% EtOAc/hexanes + 1% AcOH followed by 0-10% MeOH/CH2Cl2 as the eluent) to afford the title compound as a pale-yellow solid (0.077 g, 76% yield). The physical and spectral properties were consistent with the reported values.[59]

^{1}H NMR (400 MHz, DMSO-d_6): δ 13.42 (bs, 1H), 8.39 (s, 1H), 8.14 (d, J = 7.8 Hz, 1H), 8.05 (d, J = 8.1 Hz, 1H), 7.71 (t, J = 7.7 Hz, 1H), 7.50 (s, 2H).

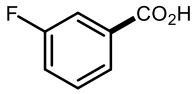

3-**fluorobenzoic acid (18):** Prepared according to the general procedure using 1-bromo-3-fluorobenzene (0.5 mmol, 56 µl, 1 equiv.), sodium formate (0.75 mmol, 0.051 g, 1.5 equiv.), 4CzIPN (.005 mmol, 0.0039 g, 1 mol%), N-phenyl-bis(trifluoromethanesulfonimide) (0.075 mmol, 0.027 g, 15 mol%), and [4,4'-Bis(1,1-dimethyl)-2,2'-bipyridine] nickel (II) bromide (0.05 mmol, 0.024 g, 10 mol%), in 1:1 DMSO/dioxane (5 mL). After 16 hours the reaction was quenched with 1M HCl (10 mL), extracted three times with ethyl acetate, dried over $MgSO_4$ and concentrated in vacuo. The crude reaction mixture was purified by silica chromatography (0-50% EtOAc/hexanes + 1% AcOH followed by 0-10% MeOH/CH2Cl2 as the eluent) to afford the title compound as a white solid (0.058 g, 84% yield). The physical and spectral properties were consistent with the reported values.[60]

^{1}H NMR (400 MHz, DMSO-d$_6$): δ 13.30 (bs, 1H), 7.80 (dt, J = 7.6, 1.3 Hz, 1H), 7.69-7.63 (m, 1H), 7.61-7.54 (m, 1H), 7.53-7.46 (m, 1H).

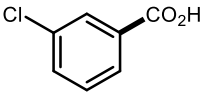

3-chlorobenzoic acid (19): Prepared according to the general procedure using 1-bromo-3-chlorobenzene (0.5 mmol, 59 µl, 1 equiv.), sodium formate (0.75 mmol, 0.051 g, 1.5 equiv.), 4CzIPN (.005 mmol, 0.0039 g, 1 mol%), N-phenyl-bis(trifluoromethanesulfonimide) (0.075 mmol, 0.027 g, 15 mol%), and [4,4'-Bis(1,1-dimethyl)-2,2'-bipyridine] nickel (II) bromide (0.05 mmol, 0.024 g, 10 mol%), in 1:1 DMSO/dioxane (5 mL). After 16 hours the reaction was quenched with 1M HCl (10 mL), extracted three times with ethyl acetate, dried over $MgSO_4$ and concentrated in vacuo. The crude reaction mixture was purified by silica chromatography (0-50% EtOAc/hexanes + 1% AcOH followed by 0-10% MeOH/CH2Cl2 as the eluent) to afford the title compound as a white solid (0.065 g, 83% yield). The physical and spectral properties were consistent with the reported values.[61]

1H NMR (400 MHz, DMSO-d6) δ 13.34 (bs, 1H), 7.93-7.89 (m, 2H), 7.74-7.69 (m, 1H), 7.55 (t, J = 8.1 Hz, 1H).

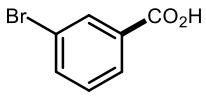

3-bromobenzoic acid (20): Prepared according to the general procedure using 1-bromo-3-iodobenzene (0.5 mmol, 64 µl, 1 equiv.), sodium formate (0.75 mmol, 0.051 g, 1.5 equiv.), 4CzIPN (.005 mmol, 0.0039 g, 1 mol%), N-phenyl-bis(trifluoromethanesulfonimide) (0.075 mmol, 0.027 g, 15 mol%), and [4,4'-Bis(1,1-dimethyl)-2,2'-bipyridine] nickel (II) bromide (0.05 mmol, 0.024 g, 10 mol%), in 1:1 DMSO/dioxane (5 mL). After 16 hours the reaction was quenched with 1M HCl (10 mL), extracted three times with ethyl acetate, dried over $MgSO_4$ and concentrated in vacuo. The crude reaction mixture was purified by silica chromatography (10-20% EtOAc/hexanes + 1% AcOH as the eluent) to afford the title compound as a light-yellow

solid (0.082 g, 82% yield). The physical and spectral properties were consistent with the reported values.[62]

^{1}H NMR (400 MHz, DMSO-d_6): δ 13.32 (bs, 1H), 8.04 (t, J = 1.8 Hz, 1H), 7.93 (dt, J = 7.8, 1.3 Hz, 1H), 7.86-7.82 (m, 1H).

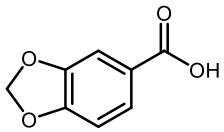

Benzo[d][1,3]dioxole-5-carboxylic acid (21): Prepared according to the general procedure using 5-bromo-1,3-benzodioxole (0.5 mmol, 60 µl, 1 equiv.), sodium formate (0.75 mmol, 0.051 g, 1.5 equiv.), 4CzIPN (.005 mmol, 0.0039 g, 1 mol%), N-phenyl-bis(trifluoromethanesulfonimide) (0.075 mmol, 0.027 g, 15 mol%), and [4,4'-Bis(1,1-dimethyl)-2,2'-bipyridine] nickel (II) bromide (0.05 mmol, 0.024 g, 10 mol%), in 1:1 DMSO/dioxane (5 mL). After 16 hours the reaction was quenched with 1M HCl (10 mL), extracted three times with ethyl acetate, dried over $MgSO_4$ and concentrated in vacuo. The crude reaction mixture was purified by silica chromatography (20-30% EtOAc/hexanes + 1% AcOH as the eluent) to afford the title compound as a white solid (0.055 g, 66% yield). The physical and spectral properties were consistent with the reported values.[63]

^{1}H NMR (400 MHz, DMSO-d_6): δ 12.76 (s, 1H), 7.54 (dd, J = 8.3, 1.7 Hz, 1H), 7.36 (d, J = 1.7 Hz, 1H), 7.00 (d, J = 8.1 Hz, 1H), 6.12 (s, 2H).

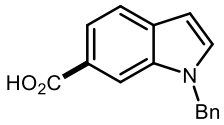

1-benzyl-1H-indole-6-carboxylic acid (22): Prepared according to the general procedure using 1-benzyl-6-bromo-1H-indole (0.5 mmol, 0.143 g, 1 equiv.), sodium formate (0.75 mmol, 0.051 g, 1.5 equiv.), 4CzIPN (.005 mmol, 0.0039 g, 1 mol%), N-phenyl-bis(trifluoromethanesulfonimide) (0.075 mmol, 0.027 g, 15 mol%), and [4,4'-Bis(1,1-dimethyl)-2,2'-bipyridine] nickel (II) bromide (0.05 mmol, 0.024 g, 10 mol%), in 1:1 DMSO/dioxane (5 mL). After 16 hours the reaction was quenched with 1M HCl (10 mL), extracted three times with ethyl acetate, dried over $MgSO_4$ and concentrated in vacuo. The crude reaction mixture was purified by silica chromatography (10-30% EtOAc/hexanes + 1% AcOH as the eluent) to afford the title compound as a light-yellow solid (0.063 g, 50% yield). The physical and spectral properties were consistent with the reported values.

^{1}H NMR (400 MHz, DMSO-d_6): δ 12.57 (bs, 1H), 8.05-8.04 (m, 1H), 7.77 (d, J = 3.0 Hz, 1H), 7.63-7.61 (m, 2H), 7.31 (t, J = 7.1 Hz, 2H), 7.25 (t, J = 7.4 Hz, 1H), 7.16 (d, J = 7.4 Hz, 2H), 6.59 (dd, J = 3.1, 0.9 Hz, 1H), 5.53 (s, 2H).

^{13}C NMR (100 MHz, DMSO-d_6): δ 168.22, 138.07. 135.05, 132.78, 131.80, 128.63, 127.41, 126.74, 123.47, 120.17, 120.11, 112.18, 101.39, 49f.16.

HRMS (APCI) m/z: [M+H] calcd. for C16H14O2N, 252.1019, found 252.1015.

R_f: 0.49 (30% EtOAc/Hexanes + 1% AcOH).

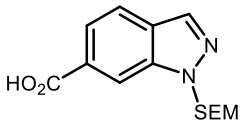

1-((2-(trimethylsilyl)ethoxy)methyl)-1H-indazole-6-carboxylic acid (23): Prepared according to the general procedure using S5 (0.5 mmol, 0.143 g, 1 equiv.), sodium formate (0.75 mmol, 0.051 g, 1.5 equiv.), 4CzIPN (.005 mmol, 0.0039 g, 1 mol%), N-phenyl-bis(trifluoromethanesulfonimide) (0.075 mmol, 0.027 g, 15 mol%), and [4,4'-Bis(1,1-dimethyl)-2,2'-bipyridine] nickel (II) bromide (0.05 mmol, 0.024 g, 10 mol%), in 1:1 DMSO/dioxane (5 mL). After 16 hours the reaction was quenched with 1M HCl (10 mL), extracted three times with ethyl acetate, dried over $MgSO_4$ and concentrated in vacuo. The crude reaction mixture was purified by silica chromatography (10-30% EtOAc/hexanes + 1% AcOH as the eluent) to afford the title compound as a light-yellow solid (0.066 g, 66% yield). The physical and spectral properties were consistent with the reported values.

^{1}H NMR (400 MHz, DMSO-d$_6$): δ 13.13 (bs, 1H), 8.35 (d, J = 1.1 Hz, 1H), 8.25 (d, J = 1.0 Hz, 1H), 7.89 (dd, J = 8.5, 0.8Hz, 1H), 7.75 (dd, J = 8.4, 1.3 Hz, 1H), 5.85 (s, 2H), 3.51 (t, J = 8.1 Hz, 2H), 0.79 (t, J = 7.9 Hz, 2H), -0.13 (s, 9H).

^{13}C NMR: (400 MHz, DMSO-d6) δ 167.52, 139.15, 134.05, 128.96, 126.66, 121.46, 121.04, 112.02, 76.96, 65.65, 17.11, -1.21, -1.47, -1.72.

HRMS (APCI) m/z: [M+H] calcd. for C14H21O3N2Si, 293.1316, found 293.1313.

R$_f$: 0.52 (30% EtOAc/Hexanes + 1% AcOH).

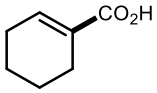

Cyclohex-1-ene-1-carboxylic acid (24): Prepared according to the general procedure S3 (0.1 mmol, 12 µl, 1 equiv.), sodium formate (0.15 mmol, 0.010 g, 1.5 equiv.), 4CzIPN (.0001 mmol, 0.0008 g, 1 mol%), N-phenyl-bis(trifluoromethanesulfonimide) (0.015 mmol, 0.0053 g, 15 mol%), and [4,4'-Bis(1,1-dimethyl)-2,2'-bipyridine] nickel (II) bromide (0.01 mmol, 0.0048 g, 10 mol%), in 1:1 DMSO/dioxane (5 mL). After 16 hours the reaction was quenched with 1M HCl (10 mL), extracted three times with ethyl acetate, dried over $MgSO_4$ and concentrated in vacuo. Dibromomethane (0.1 mmol, 7.0 µl, 1.0 equiv.) was added to the crude reaction mixture as an internal standard and the sample was analyzed via ^{1}H NMR (d = 5 s), and the integral values were used to calculate product yield (80% yield by NMR).[64]

V. NMR Spectra

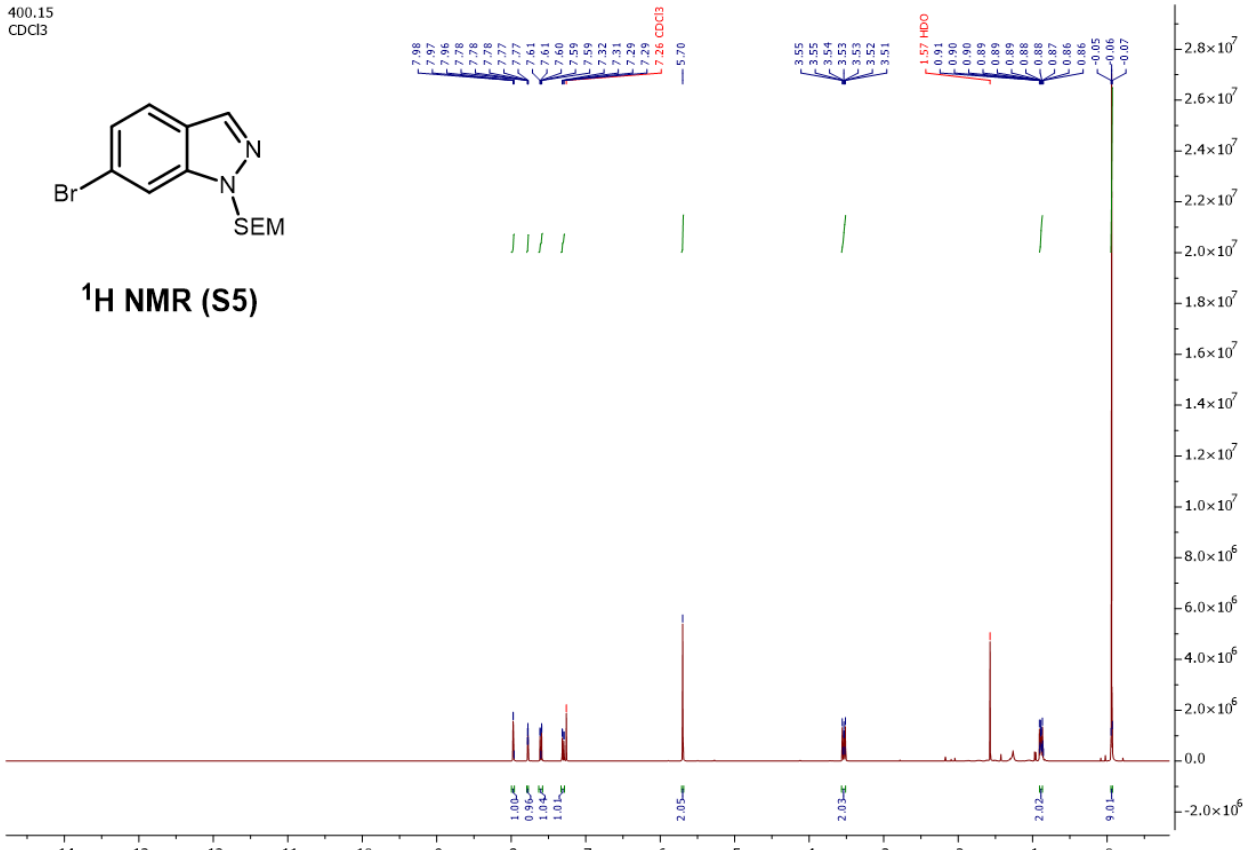

^{1}H NMR (S5)

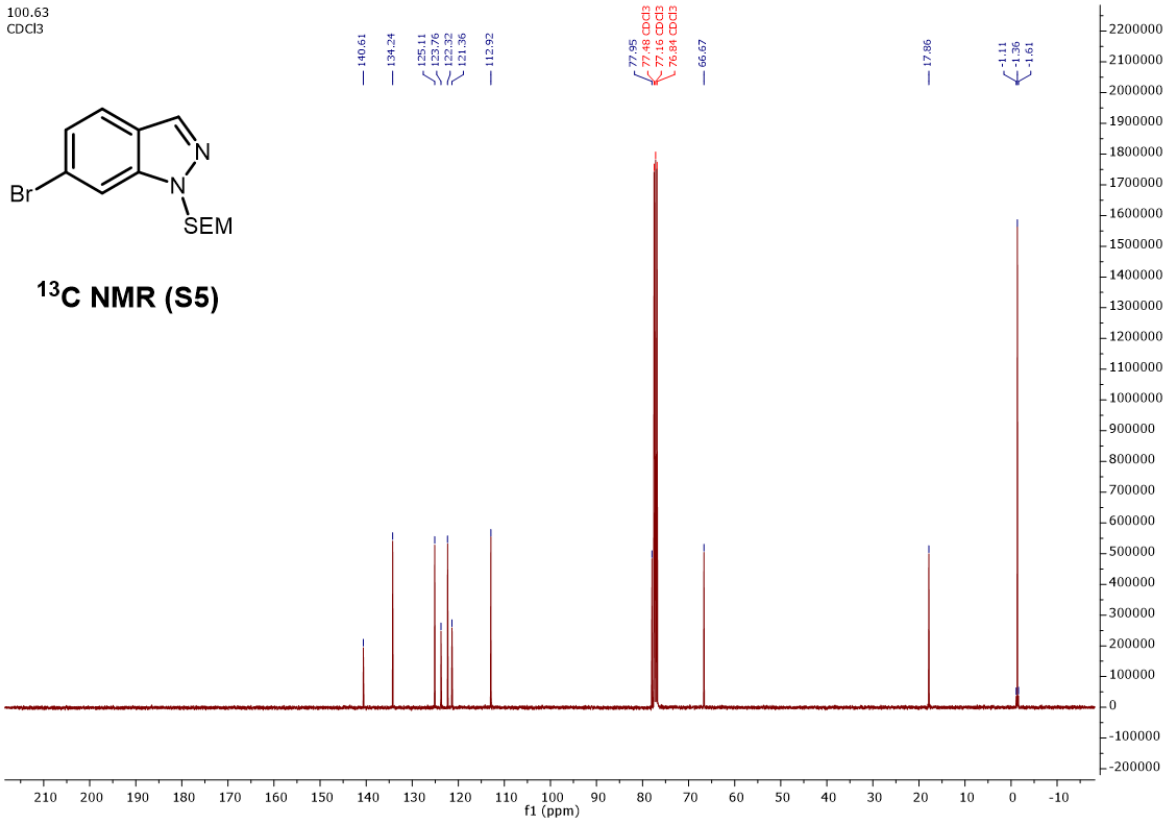

^{13}C NMR (S5)

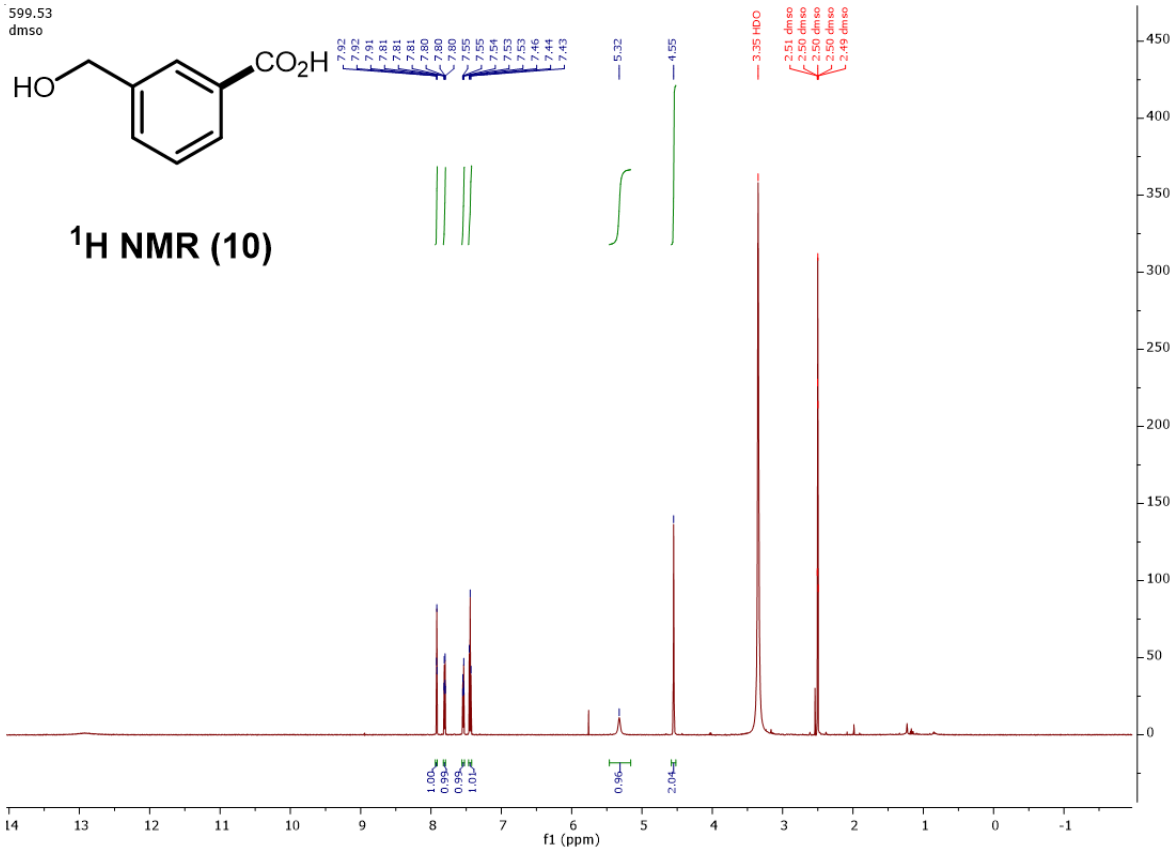
599.53
dmso
HO
CO2H
1H NMR (10)
7.92
7.92
7.91
7.81
7.81
7.81
7.80
7.80
7.80
7.55
7.55
7.54
7.53
7.53
7.46
7.44
7.43
5.32
4.55
3.35 HDO
2.51 dmso
2.50 dmso
2.50 dmso
2.50 dmso
2.49 dmso
1.00
0.99
0.99
1.01
0.96
2.04
f1 (ppm)

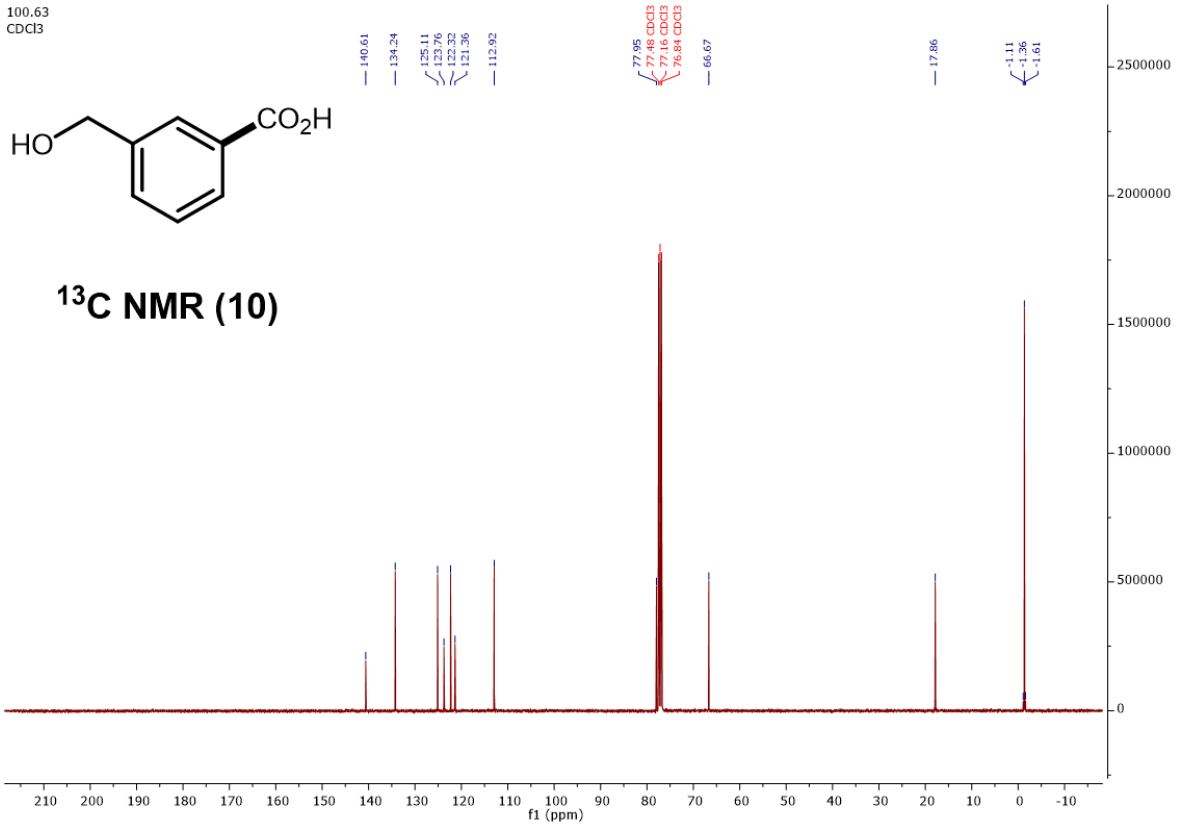
100.63
CDCl3
HO
CO2H
13C NMR (10)
140.61
134.24
125.11
123.76
122.32
121.36
112.92
77.95
77.48 CDCl3
77.16 CDCl3
76.84 CDCl3
66.67
17.86
1.11
1.36
1.61
f1 (ppm)

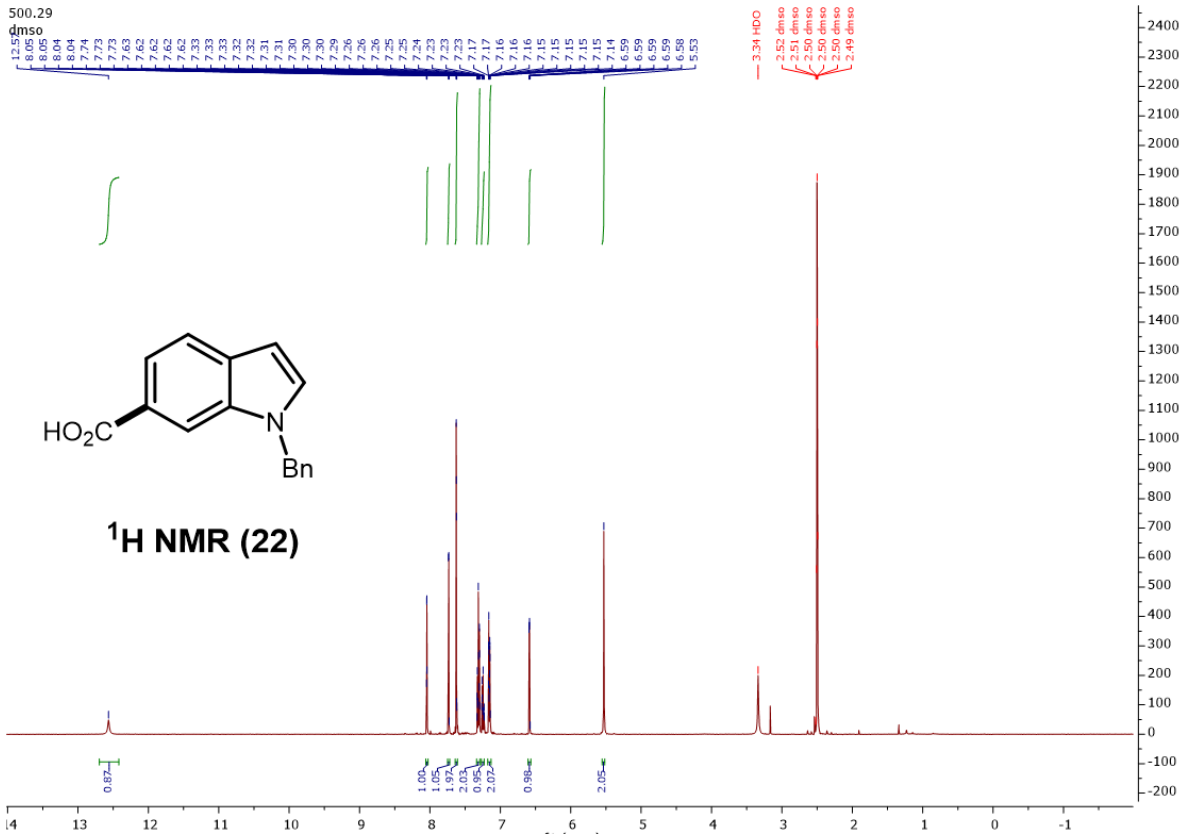
500.29
dmso
HO2C
N
Bn
1H NMR (22)

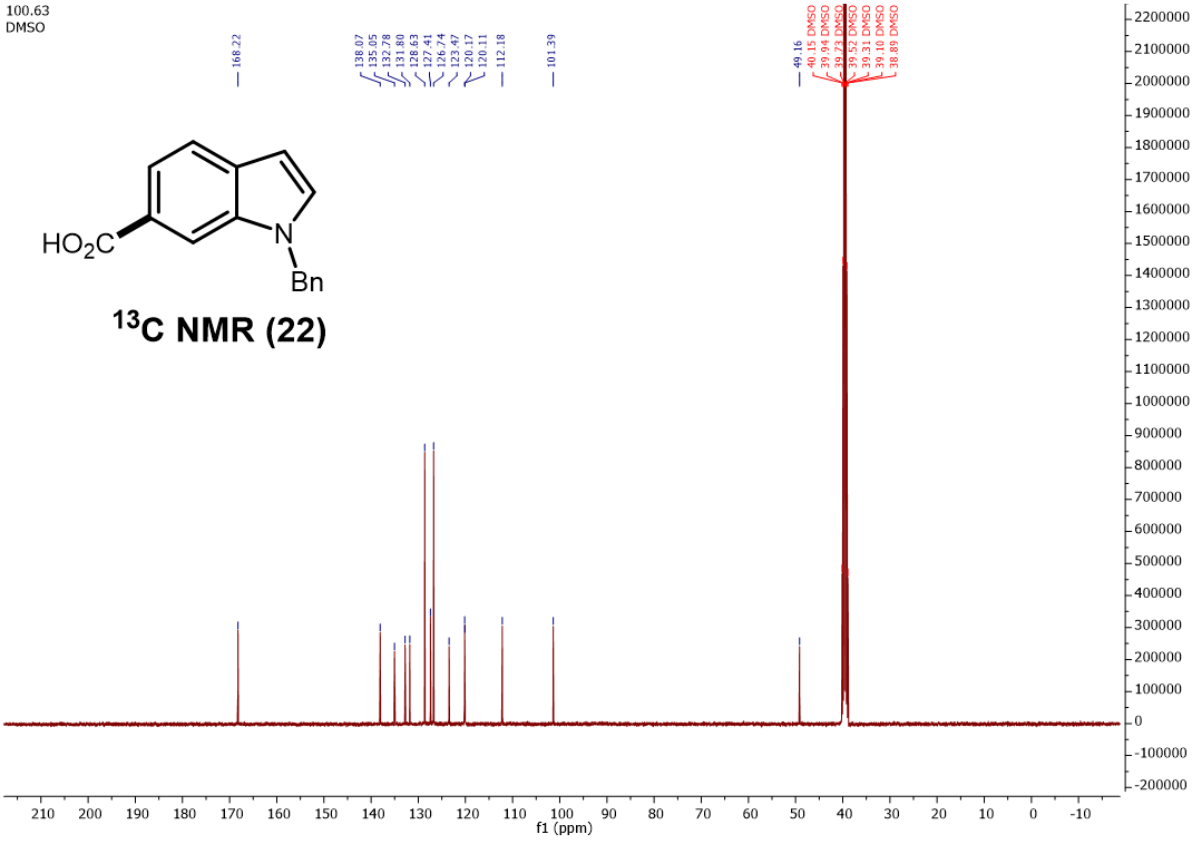
100.63
DMSO
HO2C
N
Bn
13C NMR (22)
f1 (ppm)

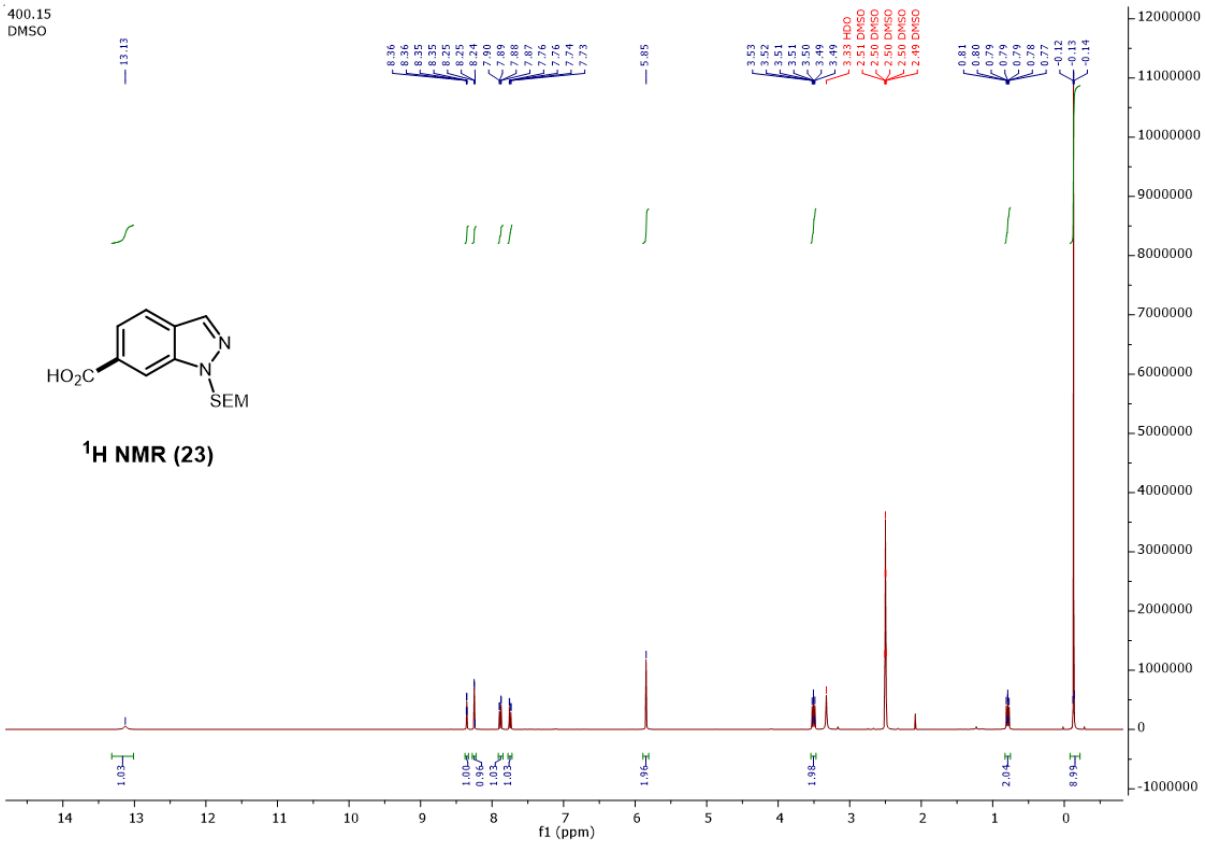

^{1}H NMR (23)

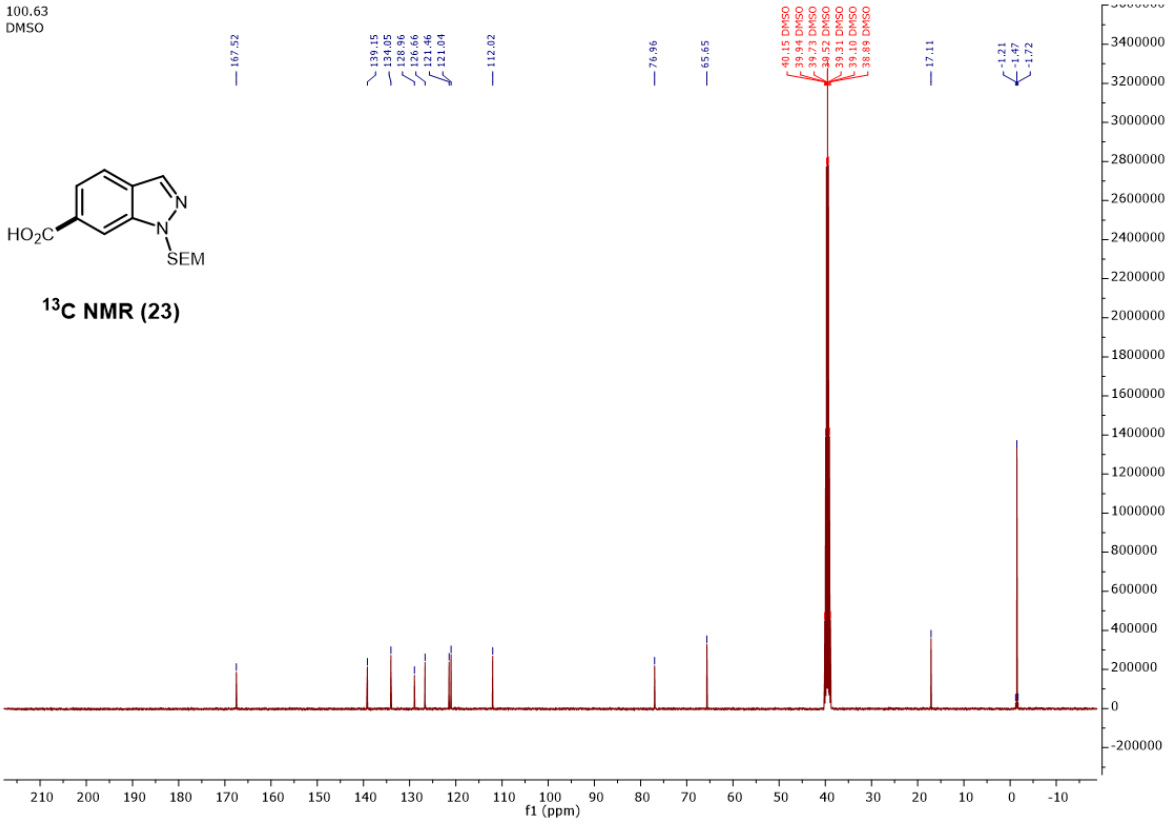

^{13}C NMR (23)

References

(1) Danishefsky, S. J. Reflections on Organic Synthesis: The Evolution of a General Strategy for the Stereoselective Construction of Polyoxygenated Natural Products. *Aldrichimica Acta* **1986**, *19*, 59.

(2) Hoffmann, R. W. Natural Product Synthesis: Changes over Time. *Angew. Chem. Int. Ed.* **2013**, *52* (1), 123–130. https://doi.org/10.1002/anie.201203319.

(3) Woodward, R. B.; Cava, M. P.; Ollis, W. D.; Hunger, A.; Daeniker, H. U.; Schenker, K. THE TOTAL SYNTHESIS OF STRYCHNINE. *J. Am. Chem. Soc.* **1954**, *76* (18), 4749–4751. https://doi.org/10.1021/ja01647a088.

(4) Woodward, R. B.; Cava, M. P.; Ollis, W. D.; Hunger, A.; Daeniker, H. U.; Schenker, K. The Total Synthesis of Strychnine. *Tetrahedron* **1963**, *19* (2), 247–288. https://doi.org/10.1016/S0040-4020(01)98529-1.

(5) Shaw, M. H.; Twilton, J.; MacMillan, D. W. C. Photoredox Catalysis in Organic Chemistry. *J. Org. Chem.* **2016**, *81* (16), 6898–6926. https://doi.org/10.1021/acs.joc.6b01449.

(6) Prier, C. K.; Rankic, D. A.; MacMillan, D. W. C. Visible Light Photoredox Catalysis with Transition Metal Complexes: Applications in Organic Synthesis. *Chem. Rev.* **2013**, *113* (7), 5322–5363. https://doi.org/10.1021/cr300503r.

(7) Narayanam, J. M. R.; Stephenson, C. R. J. Visible Light Photoredox Catalysis: Applications in Organic Synthesis. *Chem. Soc. Rev.* **2010**, *40* (1), 102–113. https://doi.org/10.1039/B913880N.

(8) Reckenthäler, M.; Griesbeck, A. G. Photoredox Catalysis for Organic Syntheses. *Adv. Synth. Catal.* **2013**, *355* (14–15), 2727–2744. https://doi.org/10.1002/adsc.201300751.

(9) Romero, N. A.; Nicewicz, D. A. Organic Photoredox Catalysis. *Chem. Rev.* **2016**, *116* (17), 10075–10166. https://doi.org/10.1021/acs.chemrev.6b00057.

(10) Xuan, J.; Xiao, W.-J. Visible-Light Photoredox Catalysis. *Angew. Chem. Int. Ed.* **2012**, *51* (28), 6828–6838. https://doi.org/10.1002/anie.201200223.

(11) Skubi, K. L.; Blum, T. R.; Yoon, T. P. Dual Catalysis Strategies in Photochemical Synthesis. *Chem. Rev.* **2016**, *116* (17), 10035–10074. https://doi.org/10.1021/acs.chemrev.6b00018.

(12) Schultz, D. M.; Yoon, T. P. Solar Synthesis: Prospects in Visible Light Photocatalysis. *Science* **2014**, *343* (6174), 1239176. https://doi.org/10.1126/science.1239176.

(13) Sharpless, K. B. Searching for New Reactivity, 2001. https://www.nobelprize.org/prizes/chemistry/2001/sharpless/lecture/.

(14) Campagna, S.; Puntoriero, F.; Nastasi, F.; Bergamini, G.; Balzani, V. Photochemistry and Photophysics of Coordination Compounds: Ruthenium. In *Photochemistry and Photophysics of Coordination Compounds I*; Balzani, V., Campagna, S., Eds.; Topics in Current Chemistry; Springer: Berlin, Heidelberg, 2007; pp 117–214. https://doi.org/10.1007/128_2007_133.

(15) Kalyanasundaram, K. Photophysics, Photochemistry and Solar Energy Conversion with Tris(Bipyridyl)Ruthenium(II) and Its Analogues. *Coord. Chem. Rev.* **1982**, *46*, 159–244. https://doi.org/10.1016/0010-8545(82)85003-0.

(16) McCusker, J. K. Femtosecond Absorption Spectroscopy of Transition Metal Charge-Transfer Complexes. *Acc. Chem. Res.* **2003**, *36* (12), 876–887. https://doi.org/10.1021/ar030111d.

(17) Bock, C. R.; Connor, J. A.; Gutierrez, A. R.; Meyer, T. J.; Whitten, D. G.; Sullivan, B. P.; Nagle, J. K. Estimation of Excited-State Redox Potentials by Electron-Transfer Quenching. Application of Electron-Transfer Theory to Excited-State Redox Processes. *J. Am. Chem. Soc.* **1979**, *101* (17), 4815–4824. https://doi.org/10.1021/ja00511a007.

(18) Nicewicz, D. A.; Nguyen, T. M. Recent Applications of Organic Dyes as Photoredox Catalysts in Organic Synthesis. *ACS Catal.* **2014**, *4* (1), 355–360. https://doi.org/10.1021/cs400956a.

(19) Shang, T.-Y.; Lu, L.-H.; Cao, Z.; Liu, Y.; He, W.-M.; Yu, B. Recent Advances of 1,2,3,5-Tetrakis(Carbazol-9-Yl)-4,6-Dicyanobenzene (4CzIPN) in Photocatalytic Transformations. *Chem. Commun.* **2019**, *55* (38), 5408–5419. https://doi.org/10.1039/C9CC01047E.

(20) Ravelli, D.; Fagnoni, M.; Albini, A. Photoorganocatalysis. What For? *Chem. Soc. Rev.* **2012**, *42* (1), 97–113. https://doi.org/10.1039/C2CS35250H.

(21) Dias, F. B.; Santos, J.; Graves, D. R.; Data, P.; Nobuyasu, R. S.; Fox, M. A.; Batsanov, A. S.; Palmeira, T.; Berberan-Santos, M. N.; Bryce, M. R.; Monkman, A. P. The Role of Local Triplet Excited States and D-A Relative Orientation in Thermally Activated Delayed Fluorescence: Photophysics and Devices. *Adv. Sci.* **2016**, *3* (12), 1600080. https://doi.org/10.1002/advs.201600080.

(22) Turro, N. J.; Ramamurthy, V.; Scaiano, J. C. *Principles of Molecular Photochemistry: An Introduction*; University Science Books: Sausalito, Calif., 2009.

(23) Ischay, M. A.; Anzovino, M. E.; Du, J.; Yoon, T. P. Efficient Visible Light Photocatalysis of [2+2] Enone Cycloadditions. *J. Am. Chem. Soc.* **2008**, *130* (39), 12886–12887. https://doi.org/10.1021/ja805387f.

(24) Nicewicz, D. A.; MacMillan, D. W. C. Merging Photoredox Catalysis with Organocatalysis: The Direct Asymmetric Alkylation of Aldehydes. *Science* **2008**, *322* (5898), 77–80. https://doi.org/10.1126/science.1161976.

(25) Narayanam, J. M. R.; Tucker, J. W.; Stephenson, C. R. J. Electron-Transfer Photoredox Catalysis: Development of a Tin-Free Reductive Dehalogenation Reaction. *J. Am. Chem. Soc.* **2009**, *131* (25), 8756–8757. https://doi.org/10.1021/ja9033582.

(26) Ertl, P.; Altmann, E.; McKenna, J. M. The Most Common Functional Groups in Bioactive Molecules and How Their Popularity Has Evolved over Time. *J. Med. Chem.* **2020**, *63* (15), 8408–8418. https://doi.org/10.1021/acs.jmedchem.0c00754.

(27) Maag, H. Prodrugs of Carboxylic Acids. In *Prodrugs: Challenges and Rewards Part 1*; Stella, V. J., Borchardt, R. T., Hageman, M. J., Oliyai, R., Maag, H., Tilley, J. W., Eds.; Biotechnology: Pharmaceutical Aspects; Springer: New York, NY, 2007; pp 703–729. https://doi.org/10.1007/978-0-387-49785-3_20.

(28) Gooßen, L. J.; Rodríguez, N.; Gooßen, K. Carboxylic Acids as Substrates in Homogeneous Catalysis. *Angew. Chem. Int. Ed.* **2008**, *47* (17), 3100–3120. https://doi.org/10.1002/anie.200704782.

(29) Tortajada, A.; Juliá-Hernández, F.; Börjesson, M.; Moragas, T.; Martin, R. Transition-Metal-Catalyzed Carboxylation Reactions with Carbon Dioxide. *Angew. Chem. Int. Ed.* **2018**, *57* (49), 15948–15982. https://doi.org/10.1002/anie.201803186.

(30) Correa, A.; Martín, R. Palladium-Catalyzed Direct Carboxylation of Aryl Bromides with Carbon Dioxide. *J. Am. Chem. Soc.* **2009**, *131* (44), 15974–15975. https://doi.org/10.1021/ja905264a.

(31) Börjesson, M.; Moragas, T.; Martin, R. Ni-Catalyzed Carboxylation of Unactivated Alkyl Chlorides with CO2. *J. Am. Chem. Soc.* **2016**, *138* (24), 7504–7507. https://doi.org/10.1021/jacs.6b04088.

(32) Shimomaki, K.; Murata, K.; Martin, R.; Iwasawa, N. Visible-Light-Driven Carboxylation of Aryl Halides by the Combined Use of Palladium and Photoredox Catalysts. *J. Am. Chem. Soc.* **2017**, *139* (28), 9467–9470. https://doi.org/10.1021/jacs.7b04838.

(33) Shimomaki, K.; Nakajima, T.; Caner, J.; Toriumi, N.; Iwasawa, N. Palladium-Catalyzed Visible-Light-Driven Carboxylation of Aryl and Alkenyl Triflates by Using Photoredox Catalysts. *Org. Lett.* **2019**, *21* (12), 4486–4489. https://doi.org/10.1021/acs.orglett.9b01340.

(34) Hendy, C. M.; Smith, G. C.; Xu, Z.; Lian, T.; Jui, N. T. Radical Chain Reduction via Carbon Dioxide Radical Anion (CO2•–). *J. Am. Chem. Soc.* **2021**, *143* (24), 8987–8992. https://doi.org/10.1021/jacs.1c04427.

(35) Tellis, J. C.; Kelly, C. B.; Primer, D. N.; Jouffroy, M.; Patel, N. R.; Molander, G. A. Single-Electron Transmetalation via Photoredox/Nickel Dual Catalysis: Unlocking a New Paradigm for Sp3–Sp2 Cross-Coupling. *Acc. Chem. Res.* **2016**, *49* (7), 1429–1439. https://doi.org/10.1021/acs.accounts.6b00214.

(36) Tasker, S. Z.; Standley, E. A.; Jamison, T. F. Recent Advances in Homogeneous Nickel Catalysis. *Nature* **2014**, *509* (7500), 299–309. https://doi.org/10.1038/nature13274.

(37) Simoes, J. A. M.; Beauchamp, J. L. Transition Metal-Hydrogen and Metal-Carbon Bond Strengths: The Keys to Catalysis. *Chem. Rev.* **1990**, *90* (4), 629–688. https://doi.org/10.1021/cr00102a004.

(38) Engle, S. Preparation of 2,4,5,6-Tetra(9H-Carbazol-9-Yl)Isophthalonitrile. *Org. Synth.* **2019**, *96*, 455–473. https://doi.org/10.15227/orgsyn.096.0455.

(39) Speckmeier, E.; Fischer, T. G.; Zeitler, K. A Toolbox Approach To Construct Broadly Applicable Metal-Free Catalysts for Photoredox Chemistry: Deliberate Tuning of Redox

Potentials and Importance of Halogens in Donor–Acceptor Cyanoarenes. *J. Am. Chem. Soc.* **2018**, *140* (45), 15353–15365. https://doi.org/10.1021/jacs.8b08933.

(40) Zhang, X.; MacMillan, D. W. C. Direct Aldehyde C–H Arylation and Alkylation via the Combination of Nickel, Hydrogen Atom Transfer, and Photoredox Catalysis. *J. Am. Chem. Soc.* **2017**, *139* (33), 11353–11356. https://doi.org/10.1021/jacs.7b07078.

(41) Gisbertz, S.; Reischauer, S.; Pieber, B. Overcoming Limitations in Dual Photoredox/Nickel-Catalysed C–N Cross-Couplings Due to Catalyst Deactivation. *Nat. Catal.* **2020**, *3* (8), 611–620. https://doi.org/10.1038/s41929-020-0473-6.

(42) Dorsheimer, J. R.; Ashley, M. A.; Rovis, T. Dual Nickel/Photoredox-Catalyzed Deaminative Cross-Coupling of Sterically Hindered Primary Amines. *J. Am. Chem. Soc.* **2021**, *143* (46), 19294–19299. https://doi.org/10.1021/jacs.1c10150.

(43) Kawamata, Y.; Vantourout, J. C.; Hickey, D. P.; Bai, P.; Chen, L.; Hou, Q.; Qiao, W.; Barman, K.; Edwards, M. A.; Garrido-Castro, A. F.; deGruyter, J. N.; Nakamura, H.; Knouse, K.; Qin, C.; Clay, K. J.; Bao, D.; Li, C.; Starr, J. T.; Garcia-Irizarry, C.; Sach, N.; White, H. S.; Neurock, M.; Minteer, S. D.; Baran, P. S. Electrochemically Driven, Ni-Catalyzed Aryl Amination: Scope, Mechanism, and Applications. *J. Am. Chem. Soc.* **2019**, *141* (15), 6392–6402. https://doi.org/10.1021/jacs.9b01886.

(44) Oderinde, M. S.; Frenette, M.; Robbins, D. W.; Aquila, B.; Johannes, J. W. Photoredox Mediated Nickel Catalyzed Cross-Coupling of Thiols With Aryl and Heteroaryl Iodides via Thiyl Radicals. *J. Am. Chem. Soc.* **2016**, *138* (6), 1760–1763. https://doi.org/10.1021/jacs.5b11244.

(45) Xu, T.; Zhou, X.; Xiao, X.; Yuan, Y.; Liu, L.; Huang, T.; Li, C.; Tang, Z.; Chen, T. Nickel-Catalyzed Decarbonylative Thioetherification of Carboxylic Acids with Thiols. *J. Org. Chem.* **2022**, *87* (13), 8672–8684. https://doi.org/10.1021/acs.joc.2c00866.

(46) Liu, S.; Jin, S.; Wang, H.; Qi, Z.; Hu, X.; Qian, B.; Huang, H. Nickel-Catalyzed Oxidative Dehydrogenative Coupling of Alkane with Thiol for C(Sp3)-S Bond Formation. *Tetrahedron Lett.* **2021**, *68*, 152950. https://doi.org/10.1016/j.tetlet.2021.152950.

(47) Roth, H. G.; Romero, N. A.; Nicewicz, D. A. Experimental and Calculated Electrochemical Potentials of Common Organic Molecules for Applications to Single-Electron Redox Chemistry. *Synlett* **2016**, *27* (05), 714–723. https://doi.org/10.1055/s-0035-1561297.

(48) Shi, S.; Lalancette, R.; Szostak, R.; Szostak, M. Triflamides: Highly Reactive, Electronically Activated N-Sulfonyl Amides in Catalytic N–C(O) Amide Cross-Coupling. *Org. Lett.* **2019**, *21* (5), 1253–1257. https://doi.org/10.1021/acs.orglett.8b03901.

(49) Zhang, X.-L.; Guo, R.-L.; Wang, M.-Y.; Zhao, B.-Y.; Jia, Q.; Yang, J.-H.; Wang, Y.-Q. Palladium-Catalyzed Three-Component Regioselective Dehydrogenative Coupling of Indoles, 2-Methylbut-2-Ene, and Carboxylic Acids. *Org. Lett.* **2021**, *23* (24), 9574–9579. https://doi.org/10.1021/acs.orglett.1c03776.

(50) Ojha, D. P.; Prabhu, K. R. Regioselective Synthesis of Vinyl Halides, Vinyl Sulfones, and Alkynes: A Tandem Intermolecular Nucleophilic and Electrophilic Vinylation of Tosylhydrazones. *Org. Lett.* **2015**, *17* (1), 18–21. https://doi.org/10.1021/ol503114n.

(51) Tang, S.; Rauch, M.; Montag, M.; Diskin-Posner, Y.; Ben-David, Y.; Milstein, D. Catalytic Oxidative Deamination by Water with H2 Liberation. *J. Am. Chem. Soc.* **2020**, *142* (49), 20875–20882. https://doi.org/10.1021/jacs.0c10826.

(52) Farizyan, M.; Mondal, A.; Mal, S.; Deufel, F.; van Gemmeren, M. Palladium-Catalyzed Nondirected Late-Stage C–H Deuteration of Arenes. *J. Am. Chem. Soc.* **2021**, *143* (40), 16370–16376. https://doi.org/10.1021/jacs.1c08233.

(53) Kim, S. M.; Kim, D. W.; Yang, J. W. Transition-Metal-Free and Chemoselective NaOtBu–O2-Mediated Oxidative Cleavage Reactions of Vic-1,2-Diols to Carboxylic Acids and Mechanistic Insight into the Reaction Pathways. *Org. Lett.* **2014**, *16* (11), 2876–2879. https://doi.org/10.1021/ol501012f.

(54) Wang, Y.; Zhao, Z.; Pan, D.; Wang, S.; Jia, K.; Ma, D.; Yang, G.; Xue, X.-S.; Qiu, Y. Metal-Free Electrochemical Carboxylation of Organic Halides in the Presence of Catalytic Amounts of an Organomediator. *Angew. Chem. Int. Ed Engl.* **2022**, *61* (41), e202210201. https://doi.org/10.1002/anie.202210201.

(55) Ma, C.; Zhao, C.-Q.; Xu, X.-T.; Li, Z.-M.; Wang, X.-Y.; Zhang, K.; Mei, T.-S. Nickel-Catalyzed Carboxylation of Aryl and Heteroaryl Fluorosulfates Using Carbon Dioxide. *Org. Lett.* **2019**, *21* (7), 2464–2467. https://doi.org/10.1021/acs.orglett.9b00836.

(56) Shih, Y.-L.; Wu, Y.-K.; Hyodo, M.; Ryu, I. Photocatalytic Oxidative Cleavage of Alkenes by Molecular Oxygen: Reaction Scope, Mechanistic Insights, and Flow Application. *J. Org. Chem.* **2022**. https://doi.org/10.1021/acs.joc.2c02429.

(57) Liu, W.; Wang, H.; Li, C.-J. Metal-Free Markovnikov-Type Alkyne Hydration under Mild Conditions. *Org. Lett.* **2016**, *18* (9), 2184–2187. https://doi.org/10.1021/acs.orglett.6b00801.

(58) Wise, D. E.; Gogarnoiu, E. S.; Duke, A. D.; Paolillo, J. M.; Vacala, T. L.; Hussain, W. A.; Parasram, M. Photoinduced Oxygen Transfer Using Nitroarenes for the Anaerobic Cleavage of Alkenes. *J. Am. Chem. Soc.* **2022**, *144* (34), 15437–15442. https://doi.org/10.1021/jacs.2c05648.

(59) Weidel, E.; de Jong, J. C.; Brengel, C.; Storz, M. P.; Braunshausen, A.; Negri, M.; Plaza, A.; Steinbach, A.; Müller, R.; Hartmann, R. W. Structure Optimization of 2-Benzamidobenzoic Acids as PqsD Inhibitors for Pseudomonas Aeruginosa Infections and Elucidation of Binding Mode by SPR, STD NMR, and Molecular Docking. *J. Med. Chem.* **2013**, *56* (15), 6146–6155. https://doi.org/10.1021/jm4006302.

(60) Xia, A.; Qi, X.; Mao, X.; Wu, X.; Yang, X.; Zhang, R.; Xiang, Z.; Lian, Z.; Chen, Y.; Yang, S. Metal-Free Aerobic Oxidative Selective C–C Bond Cleavage in Heteroaryl-Containing

Primary and Secondary Alcohols. *Org. Lett.* **2019**, *21* (9), 3028–3033. https://doi.org/10.1021/acs.orglett.9b00563.

(61) Zhang, Z.; Zhang, G.; Xiong, N.; Xue, T.; Zhang, J.; Bai, L.; Guo, Q.; Zeng, R. Oxidative α-C–C Bond Cleavage of 2° and 3° Alcohols to Aromatic Acids with O2 at Room Temperature via Iron Photocatalysis. *Org. Lett.* **2021**, *23* (8), 2915–2920. https://doi.org/10.1021/acs.orglett.1c00556.

(62) Wang, W.; Yang, X.; Dai, R.; Yan, Z.; Wei, J.; Dou, X.; Qiu, X.; Zhang, H.; Wang, C.; Liu, Y.; Song, S.; Jiao, N. Catalytic Electrophilic Halogenation of Arenes with Electron-Withdrawing Substituents. *J. Am. Chem. Soc.* **2022**, *144* (29), 13415–13425. https://doi.org/10.1021/jacs.2c06440.

(63) Ou, J.; Tan, H.; He, S.; Wang, W.; Hu, B.; Yu, G.; Liu, K. 1,2-Dibutoxyethane-Promoted Oxidative Cleavage of Olefins into Carboxylic Acids Using O2 Under Clean Conditions. *J. Org. Chem.* **2021**, *86* (21), 14974–14982. https://doi.org/10.1021/acs.joc.1c01701.

(64) Monda, F.; Madsen, R. Zinc Oxide-Catalyzed Dehydrogenation of Primary Alcohols into Carboxylic Acids. *Chem. – Eur. J.* **2018**, *24* (67), 17832–17837. https://doi.org/10.1002/chem.201804402.